Reprint from Journal of Marine Research, Volume 39, 4, 1981.

The response of a linear baroclinic equatorial ocean to periodic forcing

by Mark A. Cane[1] and E. S. Sarachik[2]

ABSTRACT

This paper examines the response of the linear inviscid shallow water equations on a meridionally infinite but zonally bounded equatorial β-plane to periodic zonal forcings at a low frequency ω.

The solution is constructed out of the Kelvin mode and a finite sum of Rossby modes all of which have their turning points equatorward of the turning latitude $y_T \sim (2\omega)^{-1}$. The number of modes required is modest: the method allows us to examine the response to forcing over a wide range of periods and basin lengths characterized by the single relevant parameter $\phi = \omega X_E c^{-1}$, where X_E is the zonal basin length, and c is the Kelvin wave speed.

In order to study the effect of the meridional scale of the forcing, the responses to the simplest symmetric zonal forcing, $\exp[-1/2\ \mu y^2 + i\omega t]$, and the simplest anti-symmetric zonal forcing, $y \exp[-1/2\ \mu y^2 + i\omega t]$, are examined in detail. To facilitate the analysis an approximate evaluation of the sums is performed to give a complete, though approximate, closed form analytic solution in the simplest symmetric and anti-symmetric cases.

We find that for symmetric forcings, the amplitude of the response becomes relatively insensitive to the meridional scales of the forcing for scales greater than about ten degrees of latitude. For both symmetric and anti-symmetric forcings at $\phi \geqslant \pi/4$, we find the features predicted by Rossby ray theory (foci, caustics, and shadow zones) but we also find that the presence of the Kelvin mode in the symmetric case complicates the ray theoretic picture considerably. In addition we find that the phase propagation due to sums of modes need bear little relation to that expected for individual Rossby waves.

Some implications of this work for real oceans are discussed in the conclusion.

1. Introduction

The tropical oceans are so vast and our ability to observe them so limited that in lieu of the impossible goal of understanding the dynamics of equatorial oceans completely, we have been forced to focus our attention on a limited subset of approachable problems. We may categorize this subset temporally as follows: the steady circulation (e.g., the current-countercurrent-undercurrent system), the pe-

1. Dept. of Meteorology and Physical Oceanography, MIT, Cambridge, Massachusetts 02139, U.S.A.
2. Center for Earth and Planetary Physics, Harvard University, Cambridge, Massachusetts 02138, U.S.A.

riodic oscillations (annual, diurnal, etc.), and what we may call the spectacular anomalies (e.g., El Niño). Even the study of this restricted set of problems offers grave difficulties, for despite the excellent work of many dedicated scientists over the years, neither the atmospheric forcing nor the oceanic response on any of these temporal scales can be said to be known to an adequate degree of accuracy.

Of this subset of problems the seasonal oscillation of the oceans holds a rather unique position since the "steady" circulation is known to have major seasonal variations and El Niño is observed to be an enhancement of the normal seasonal warming off the coast of Peru. Attention has been focused still further on the seasonal variation of the thermocline since density data are taken with much greater frequency and coverage than current data. In particular, data have become available in the last few years on the seasonal response of the depth of the thermocline along the Equator. In the Atlantic, large swings of the equatorial thermocline normally in phase with the seasonal winds have been inferred (Katz *et al.*, 1977; Merle, 1980). Over much of the Pacific, however, seasonal variations in the depth of the thermocline are relatively minor (Meyers, 1979a, especially Fig. 7) with a possible in-phase response existing only at the eastern end (Tsuchiya, 1979).

The theoretical approach to understanding low latitude seasonal thermocline response remains in its infancy. Inferences about linear seasonal response (e.g., Philander, 1979) have been drawn from the solution of an entirely different problem, namely, the linear response of an equatorial ocean to a forcing impulsively switched on in time (see Cane and Sarachik, 1976, 1977, 1979). The response in this impulsive case proceeds behind Kelvin wavefronts propagating eastward and Rossby wavefronts propagating westward. Much of the response of the ocean occurs after a single Kelvin and Rossby wavefront has crossed the basin. By analogy, therefore, it was concluded that seasonal response would be "adjusted," i.e., in phase with the forcing, if the basin was small enough for a Kelvin and Rossby wavefront to cross the basin during a single forcing period. We will see below that while there is some truth to this inference that small basin size implies a thermocline response in phase with the wind, there are fundamental and profound differences between the dynamics of impulsive response and the dynamics of periodic response.

Some hint of this difference may be glimpsed by comparing the periodic response of a single mid-latitude Rossby wave (e.g., Meyers, 1979b) with the response to packets of linear mid-latitude Rossby waves (Schopf *et al.*, 1981). The ability of many Rossby waves, all oscillating at the same frequency, to constructively and destructively interfere with each other is graphically pointed to Schopf *et al.* (1981). Constructive interference manifests itself in narrow regions of enhanced periodic response ("caustics") and destructive interference in broad regions of muted response ("shadow zones"). The work of Schopf *et al.* (1981) is based on low

frequency, mid-latitude approximations that are not completely applicable to equatorial regions, but it is fundamental in illustrating the importance of dealing with *all* the modes that can oscillate at the forcing frequency—a single mode will not do.

Work on equatorial periodic response has concentrated on linear and nonlinear numerical time-stepping models spun-up from rest. Kindle (1979) uses a two-layer model with nonlinear terms retained to examine the annual and semi-annual response to some idealized winds in a square basin with the longitudinal size of the Pacific. Busalacchi and O'Brien (1980) force a linear two-layer model with the basin geometry of the Pacific with seasonal winds with no meridional dependence and with observed winds. Philander and Pacanowski (1980) force a small basin (5000 km) with idealized winds and compare the computed linear and nonlinear response for various forcing frequencies.

Finally, though not dealing explicitly with a forced problem, Moore (1968), in a thesis that laid much of the groundwork for theoretical equatorial oceanography, considered the modes of a bounded equatorial basin. In so doing, he had to consider both high and low frequency planetary waves between meridians at the east and the west, and the means of satisfying correct boundary conditions at these meridians. Much of our work will be similar to that of Moore (1968) but in confining ourselves to low frequency response, we will be able to make approximations at low frequency that considerably simplify the analysis.

In this paper we will examine the linear periodic response of a single baroclinic mode to idealized zonal forcings on a meridionally unbounded equatorial β-plane. Thus we will solve the (equatorially scaled) shallow water equations for the response at the (low) frequency ω equal to that of the forcing:

$$\begin{aligned} i\omega u - yv &= -h_x + F(y)\exp[i\omega t] \\ i\omega v + yu &= -h_y \\ i\omega h + u_x + v_y &= 0 \end{aligned} \tag{1}$$

between $x = 0$ and $x = X_E$. Our method of solution is approximate and involves summing meridional modes. This method is very efficient compared to time marching and allows us to obtain linear periodic solutions over a wide range of frequencies, basin lengths and forcings, thus inferring general properties of low frequency equatorial response.

We will concentrate on periodic variations of the height field since, in this one layer model, currents have been vertically averaged. Thus while there are currents that go with the height field variations we will describe, these currents bear but faint resemblance to the currents that would exist were the single layer of fluid to be more precisely resolved. It is an item of experience that height field variations are adequately given by the shallow water equations even when the currents are not.

We will find that a crucial parameter in the response is $\phi = \omega X_E c^{-1}$ where c is the Kelvin wave speed in the baroclinic mode of interest (Kindle, 1979): this parameter can be interpreted as the ratio of length of the basin to the distance a Kelvin wave travels in ω^{-1}. For orientation, the values of this parameter for seasonal forcing for the first and second baroclinic modes for the Atlantic are .54 and .96; for the Pacific, 1.13 and 2.05, respectively. We will find that for extremely small values of ϕ another parameter becomes important, viz. ϕ times the ratio of the meridional scale of the forcing to the equatorial radius of deformation. Even for ϕ of order unity, a sensitivity (mostly in the phase) to the meridional scale of the forcing remains. At higher values of ϕ, various resonances and other quasi-singular behaviors occur ("foci") due to the constructive and destructive interference of many modes oscillating at the same frequency ω.

The plan of this paper is as follows: In Section 2 we will examine low frequency periodic response in the barotropic vorticity equation. This model, which we have previously found helpful in our studies of impulsive response (Cane and Sarachik, 1976, 1977), will be used to examine the role of friction in producing the nondispersive long-wave approximation used extensively later in the paper. Section 3 will present a detailed derivation of the solutions to (1) in terms of sums of meridional modes for a general zonal forcing and Section 4 will not only present detailed solutions for a zonal forcing of form $F = \exp[-1/2\ \mu y^2]$ but will also explicate and illuminate these results with a complete, though necessarily approximate, analytic solution to this problem. Section 5 will present solutions for a zonal forcing anti-symmetric about the equator. In the final section, the general properties of linear, low frequency, low latitude response will be summarized and, on the basis of this summary, some points relevant to the ocean and to some numerical models of the ocean will be raised. Mathematical details and a review of notation employed in the body of the text are relegated to the Appendices.

2. Periodic response in the barotropic vorticity equation

Because the dispersive properties of the barotropic vorticity equation are quite similar to those of equatorial Rossby waves, the barotropic vorticity equation proves to be a particularly convenient theoretical laboratory for testing out approximations (e.g., Section 3 of Cane and Sarachik, 1976). In this section we will examine the effects of friction on low frequency periodic response in the barotropic vorticity equation and show that friction kills the *short* Rossby waves thereby rendering valid the long-wave approximation.

The barotropic vorticity equation in the presence of periodic forcing by an x-independent wind stress curl can be written

$$i\omega\,[\psi_{xx} - m^2\psi] + \beta\psi_x = -r\psi_{xx} + C\exp[i\omega t] \tag{2}$$

where r is a Rayleigh friction coefficient and m may be considered the meridional wavenumber. The forced solution can be written

$$\psi(x, t) = \left\{ -iC(\omega m^2)^{-1} \left[1 - \exp[-ik_+(x - X_E)] \right] + \beta_- \exp[-ik_- x] + \beta_+ \exp[-ik_+ x] \right\} \exp[i\omega t] \quad (3)$$

where β_+ and β_- are determined by the boundary conditions $\psi(0) = \psi(X_E) = 0$, and $k_\pm$ are given by the dispersion relation

$$k_\pm = -\frac{\beta}{2(\omega - ir)} \pm \frac{\beta}{2(\omega - ir)} \left[1 - \frac{4\omega m^2 (\omega - ir)^2}{\beta^2} \right]^{1/2}. \quad (4)$$

When the frequency is low enough and friction is absent, k_+ defines a long, nearly nondispersive Rossby wave with group velocity $-\beta m^{-2}$ to the west, while k_- defines a short, highly dispersive Rossby wave with short zonal wavelength, westward phase velocity, but very slow eastward group velocity $\omega^2\beta^{-1}$.

We now define the length scale $l = \omega\beta^{-1}$ (which is of order 10 km for seasonal forcing) and define a parameter $\epsilon \equiv lm$ which we will assume to be much smaller than unity. We also assume that the frictional time scale is long compared to the period of the forcing:[3] $r = \delta\omega$ where $\delta << 1$. With these assumptions, (4) becomes

$$k_+ = -\omega m^2 \beta^{-1} + 0(\epsilon^2, \delta\epsilon^2) \sim -\epsilon m$$
$$k_- = -(1 + i\delta) l^{-1} + 0(\epsilon^2, \delta\epsilon^2) \sim m\epsilon^{-1}(1 + i\delta) \; . \quad (5)$$

The zonal scale of the long Rossby is, by assumption, much longer than the meridional scale in analogy to the equatorial case. Also the zonal scale of the long Rossby wave is clearly much greater than the scale l, i.e., $k_+ l = \epsilon^2$ so that the ordering is k_+^{-1}: m^{-1}: $l = 1$: ϵ: ϵ^2. Furthermore, it is clear from (5) and (3) that the friction causes a decay of the stream-function from the western boundary with a frictional decay scale $D = \delta\epsilon m^{-1} = l\delta^{-1}$, which may be interpreted as the distance the slow Rossby waves traveling with group velocity $\omega^2\beta^{-1}$ travel in the frictional time scale r^{-1}.

There are two interesting cases, namely, when friction is so small that $D >> X_E$ and the converse case, when $D << X_E$.

The first case is essentially inviscid and both the amplitude and phase show modulation of scale l due to the short Rossby waves which propagate with small group velocity eastward into the basin.

The second case is that the frictional decay scale is small compared to the basin size, so that $\exp[ik_- X_E]$ is negligible. The streamfunction in (3) can then be written

3. This is not a necessary assumption—it simplifies the algebra for the purposes of the discussion.

$$\psi(x, t) = iC(\omega m^2)^{-1}[\exp[i\phi\xi] - 1]\exp[i\omega t]$$

$$+ iC(\omega m^2)^{-1}[1 - \exp[i\phi\xi]]\exp[-xm\epsilon^{-1}(i + \delta)]\exp[i\omega t] \quad (6)$$

where $\phi \equiv \omega X_E m^2 \beta^{-1}$ and the dimensionless parameter measuring distance from the eastern boundary is $\xi = (x - X_E)X_E^{-1}$. The parameter ϕ is the ratio of the time a nondispersive long Rossby wave (travelling at velocity $-\beta m^{-2}$) takes to cross the basin to the forcing time scale $1/\omega$. Alternately, ϕ is the ratio of the basin size to the length scale of the long Rossby wave. As we shall see below, ϕ is the crucial parameter describing the interior periodic response.

The solution (6) has an obvious interpretation. The first term is the interior response and could have been obtained by solving the nondispersive forced equation

$$-i\omega m^2\psi + \beta\psi_x = C\exp[i\omega t]$$

with the single boundary condition at the east $\psi(X_E) = 0$. The second term is the boundary layer correction at the west. The crucial point is that, just as in the classic argument of Pedlosky (1965), friction prevents the short Rossby wave (with $0(\omega^2)$ group velocity to the east) from penetrating into the interior. Even for friction so small that the decay time is as long as 10 years, D is only about 600 km (for annual waves); thus the viscous case $D << X_E$ is the one more relevant to the real oceans. In this case the interior response is totally determined by the long Rossby wave (with group velocity and phase velocity to the west). If we concentrate on the interior response therefore, we can ignore the short Rossby wave altogether; its only role is to satisfy the boundary condition at $x = 0$. We see that small amounts of friction are sufficient to eliminate the short Rossby waves—the interior solution given by the long Rossby wave is identical to the long wave approximation.

The interior periodic response has its own intrinsic interest and provides the sort of intuition against which we can test the more complicated equatorial periodic response. We see immediately from the interior solution in (6) that if $\phi << 1$, the interior response is simply

$$\psi(x, t) = \beta^{-1} C(x - X_E)\exp[i\omega t]$$

and is therefore Sverdrup and in-phase with the forcing over the entire basin, i.e., for $-1 < \xi < 0$. Even if ϕ is not small, there will still be a region near the eastern boundary for which $|\phi\xi| << 1$ so that in this region the response will be in-phase and Sverdrup. Outside this region, the phase will vary monotonically across the basin. The interior solution can be rewritten as $\psi(x, t) = A\exp[-i\chi]\exp[i\omega t]$ where A is the (real) amplitude and χ is the (real) phase lag of the response with respect to the forcing. For the interior solution in (6)

$$A = 2C(\omega m^2)^{-1}\left|\sin\frac{1}{2}\phi\xi\right|$$

and

$$\chi = \arctan\left[\frac{1-\cos\phi\xi}{\sin\phi\xi}\right].$$

We see that the phase decreases monotonically from zero to -2π as the $|\phi\xi|$ goes from zero to 4π while the amplitude has zeroes at $|\phi\xi| = 2n\pi$. Thus for ξ near the points $|\phi\xi| = 4n\pi$ the response would again be in phase with the forcing but for the fact that at these same points the amplitude of the oscillations vanish.

As a final observation, we may note that for a given basin size X_E, ϕ may not be small at frequency ω but may be small at some lower frequency ω'. Thus we have the possibility that the response may not be in phase with seasonal forcing, say, but may be in phase with interannual forcing of sufficiently long period.

In this section we have considered the effect of friction on short Rossby waves and shown that in the presence of friction, these waves will not affect the interior, thereby rendering the long wave approximation valid. In the next section we will consider response on an equatorial β plane where the complications of many Rossby waves of different meridional mode numbers and of an equatorial Kelvin wave will be present.

3. The general solution on an equatorial β-plane

We wish to solve the periodic shallow water equations (1) between $x = 0$ and $x = X_E$. To do this we will construct the periodic solution in the absence of boundaries and then add sums of free Rossby and Kelvin waves oscillating at frequency ω to satisfy the boundary conditions. The boundary condition at the east is straightforward; $u = 0$ at $x = X_E$. The western boundary condition is more subtle. We have seen in the previous section that friction traps the short Rossby waves and prevents them from reaching the interior; it is therefore clear that we need not consider them further. But by no longer considering the short Rossby waves, we are no longer able to satisfy the condition $u = 0$ on the western boundary for it is the combination of short and long Rossby waves and Kelvin waves that allow this boundary condition to be satisfied (Moore, 1968). We require a boundary condition that gives the correct *long wave* reflections at the western boundary. In Cane and Sarachik (1977, p. 404) we showed that the sum of short Rossby waves formed a boundary layer which was capable of transferring zonal mass flux meridionally but which when integrated meridionally carried no net zonal mass flux. Since the meridional integral of the boundary condition $u = 0$ must necessarily vanish, and since the integral of u involving only the short Rossby waves also vanishes, the proper boundary condition for the subset of waves consisting of the Kelvin and long Rossby waves alone is:

$$\int_{-\infty}^{\infty} u\,dy = 0 \qquad \text{at } x = 0\ , \tag{7}$$

which says that all the meridionally integrated zonal mass flux incident on the western boundary is returned by the Kelvin wave.

The dispersion relation for the Kelvin wave needs no approximation since it is already nondispersive ($k_K = \omega$). The dispersion relation for the Rossby wave with group velocity to the west is

$$k_n = -(2\omega)^{-1} + [(4\omega^2)^{-1} + \omega^2 - (2n+1)]^{1/2} \ , \tag{8}$$

where, at low frequency, we may neglect ω^2 with respect to $(4\omega^2)^{-1}$. Only those meridional modes whose turning points (at $y^2 = 2n + 1$) lie equatorward of the turning point at frequency ω (defined as $y_T^2 = (4\omega^2)^{-1}$) have real wave number—all higher ones decay westward into the basin. Since only propagating waves can reach the other side to produce Kelvin waves, all sums need only be summed to N (such that $2N + 1 = y_T^2$) to satisfy the boundary conditions. The solutions will then only be valid for $|y| < |y_T|$; poleward of these points, only boundary trapped modes whose sum asymptotes to Kelvin waves exist (Moore, 1968). As a final approximation, we will assume the waves are nondispersive even up to $n = N$ so that $k_n = -(2n + 1)\omega$, $n \leqslant N$. As we will see, the amplitudes of the modes near $n = N$ are small, and these modes have a very small effect on motions in the neighborhood of the equator.

In order to construct the periodic unbounded solution, we return to the general formulation of forced baroclinic response given in Section 4 of Cane and Sarachik (1976). The general forced response (not satisfying boundary conditions) can be constructed solely out of Kelvin and Rossby modes in the long wave approximation described above. Using (44) and (47) of Cane and Sarachik (1976) we can immediately write

$$\begin{aligned}\mathbf{u}^{(1)}(x,y,t) = \sum_{n=0}^{N} \frac{1}{2\pi i} \int_{-\infty}^{\infty} \frac{r_n(k)}{k + (2n+1)\omega} \Big[&\exp[-ik(x + (2n+1)^{-1}t)] \\ &- \exp[-ikx + i\omega t] \Big] (2n+1)\mathbf{R}_n \\ + \frac{1}{2\pi i} \int_{-\infty}^{\infty} \frac{d_K}{\omega - k} \Big[&\exp[-ik(x-t)] - \exp[-ikx + i\omega t] \Big] \mathbf{M}_K \, dk \end{aligned} \tag{9}$$

where $\mathbf{R}_n$ and $\mathbf{M}_K$ are the Rossby and Kelvin modes, $d_K(k) = 2^{-1/2}(F)_0$ and $r_n(k) = (F_y)_n - (2n+1)^{-1}(yF)_n$. (The notation for the Rossby and Kelvin waves and the projections $(\ )_n$ are given in Appendix 1.) The solution in (9) gives only the zonal velocity (u) and height field (h) components; all meridional velocity components are small [$O(\omega)$].

When the forcing is independent of x, $r_n(k) = 2\pi r_n \delta(k)$, and the forced solution in (9) becomes

$$\mathbf{u}^{(1)}(y,t) = (i\omega)^{-1} \exp[i\omega t] \left\{ d_K \mathbf{M}_K + \sum_{n=0}^{N} r_n \mathbf{R}_n \right\} . \tag{10}$$

The free (long-wave) solutions needed to satisfy the boundary conditions then can be written

$$b'_K \mathbf{M}_K \exp[-i\omega x] + \sum_{n=0}^{N} a'_n \mathbf{R}_n \exp[i\omega x\,(2n+1)]$$

where $k_n = -\omega\,(2n+1)$ in the long wave approximation.

Redefining the constants b'_K and a'_n and again defining the parameters

$$\phi = \omega X_E \text{ and } \xi = (x - X_E) X_E^{-1}, \tag{11}$$

the full solution can be written in the form

$$\begin{aligned} \mathbf{u} = (i\omega)^{-1} \exp[i\omega t] \Big\{ & d_K \mathbf{M}_K [1 - \exp[-i\phi\xi]] + b_K \mathbf{M}_K \exp[-i\phi\xi] \\ & + \sum_{n=0}^{N} r_n \mathbf{R}_n (1 - \exp[i\,(2n+1)\,\phi\xi]) \\ & + \sum_{n=0}^{N} a_n \mathbf{R}_n \exp[i\,(2n+1)\,\phi\xi] \Big\} \quad . \end{aligned} \tag{12}$$

There are now $N+1$ constants (b_K and a_n) to be determined by the two boundary conditions. The parameter ϕ (dimensionally $\phi = \omega X_E c^{-1}$ where c is the Kelvin wave speed) is analogous to the parameter introduced in the previous section and will similarly prove to play a major role in the baroclinic equatorial case (see Kindle, 1979).

At the eastern boundary, $u(X_E) = 0$, so that the height at the eastern boundary h_E is independent of y equatorward of the turning points, since $yu + h_y = 0$ in the long wave approximation.

Now a result used extensively in Cane and Sarachik (1977), Eq. (23), and re-derived in (A.13), says that

$$[0, h_E]^T = h_E \pi^{1/4} \left[\mathbf{M}_K + 2 \sum \alpha_n \mathbf{R}_n \right] \tag{13}$$

where the α_n are known (A.4). At $x = X_E$, $\xi = 0$, so that the terms in (12) involving d_K and r_n are zero and comparing (12) and (13) gives

$$b_K = h_E \pi^{1/4} \text{ and } a_n = 2\alpha_n b_K \ . \tag{14}$$

We see that a single unknown parameter remains, namely the amplitude of the free Kelvin mode, b_K, which by (14) sets the amplitude of the eastern boundary height oscillations. This single parameter b_K must be determined by the western boundary condition (7) that the meridional integral of u vanish. From the definitions (A.6) we find

$$\int_{-\infty}^{\infty} (\mathbf{M}_K)_u \, dy = \pi^{1/4}; \qquad \int_{-\infty}^{\infty} (\mathbf{R}_n)_u = \pi^{1/4}\alpha_n \, [2n\,(n+1)]^{-1} \tag{15}$$

and using these relations in (12) applied to the boundary condition (7) yields

$$b_K = [1 - \exp[-2i\phi] S_N \, (\exp[2i\phi])]^{-1} \left\{ B_N \, (i\phi) + d_K \, [\exp[i\phi] - 1] \right\} \tag{16}$$

where

$$S_N \, (\exp[i\phi]) = \sum_{n=0}^{N} [n\,(n+1)]^{-1} \, (\alpha_n)^2 \exp[-in\phi] \tag{17}$$

and

$$B_N \, (i\phi) = \sum_{n=0}^{N} [2n\,(n+1)]^{-1} \, r_n \alpha_n \, (1 - \exp[-i\phi\,(2n+1)]) \; . \tag{18}$$

Finally, inserting the expressions for the a_n's and b_K (given by (14) and (16), respectively) into (12) yields the final solution for the periodic response to a periodic zonal forcing:

$$\mathbf{u} = (i\omega)^{-1} \exp[i\omega t] \left\{ d_K \mathbf{M}_K \, (1 - \exp[-i\phi\xi]) + \sum_{n=0}^{N} r_n \mathbf{R}_n \, (1 - \exp[i\phi\xi\,(2n+1)]) \right.$$

$$\left. + \, d_K \rho_N \, (i\phi) \left[\mathbf{M}_K \exp[-i\phi\xi] + \sum_{n=0}^{N} 2\alpha_{2n+1} \, \mathbf{R}_{2n+1} \exp[i\phi\xi\,(4n+3)] \right] \right\} \tag{19}$$

where

$$\rho_N \, (i\phi) = [1 - S_N \, (\exp[2i\phi]) \exp[-2i\phi]]^{-1}$$

$$\left\{ B_N \, (i\phi) \exp[-i\phi] + d_K \, (1 - \exp[-i\phi]) \right\} \; . \tag{20}$$

The solution (19) has a straightforward interpretation: the first two terms consist of the unbounded solution plus free modes directly excited at the eastern boundary. The term multiplying $\rho_N \, (i\phi)$ may be considered the Kelvin wave plus all its Rossby reflections. For y in the general vicinity of the equator, it is an excellent approximation to take $N \to \infty$ in this term (the terms in the sum decrease at least as fast as

$n^{-3/2})^4$ and the infinite sum can be performed *exactly* using the results of Appendix 2:

$$\mathbf{M}_K \exp[-i\phi\xi] + 2\sum_{n=0}^{\infty} \alpha_{2n+1}\,\mathbf{R}_{2n+1} \exp[i\phi\xi\,(4n+3)] = \exp[i\phi\xi]\,\mathbf{L}\,(y, \exp[2i\phi\xi]) \tag{21a}$$

where, by (A.9) and (A.12),

$$\exp[i\phi\xi]\,\mathbf{L}\,(y, \exp[2i\phi\xi]) = \pi^{-1/4}(\cos 2\phi\xi)^{-1/2} \exp\left[\, i\,\frac{y^2}{2}\tan 2\phi\xi \,\right] \cdot \begin{bmatrix} -i\sin 2\phi\xi \\ \cos 2\phi\xi \end{bmatrix}. \tag{21b}$$

This result was first derived by Cane and Moore (1981) and has the property that at $\phi = m\pi/2$, the sum by itself satisfies *both* boundary conditions at these values of ϕ therefore constitutes a free quasi-mode of the basin (it is not a real mode because the sum is in reality finite). The function $\rho_N\,(i\phi)$ multiplying this sum can be interpreted by noting that at $x = X_E$, only the height field remains and

$$h_E/X_E = (i\phi)^{-1} \exp[i\omega t]\pi^{-1/4}\, d_K \rho_N\,(i\phi) \tag{22}$$

where the $\xi = 0$ form of (21), has been used. We see that $\rho_N\,(i\phi)$ sets the magnitude and phase of the periodic oscillations of the height field at the eastern boundary.

Without specifying the forcing, no more can be said about the solution at this point. It is to be noted that the general solution (19) is in a form particularly suitable for computer evaluation. For the first baroclinic mode, $h \sim 65$ cm and $c \sim 2.5$ m sec^{-1} so that $N = 180$ for annual forcing. All the diagrams in the sequel are drawn directly from the computer evaluation of (19).

In the next two sections, we will examine the response to particularly simple zonal forcings over a range of ϕ and develop closed form analytic approximations to the solution.

4. Response to a symmetric zonal forcing

The symmetric zonal forcing $F = \exp[-1/2\ \mu y^2]$ has a dimensional meridional scale given by $(2\mu^{-1})^{1/2}\ L_{eq}$, where $L_{eq} = (c\beta^{-1})^{1/2}$ is the equatorial radius of deformation. This forcing is simple enough to allow a complete, though necessarily approximate, analytic solution to be obtained but general enough to allow overall conclusions about low frequency symmetric zonal forcings to be drawn. In particular, we will examine the response over a wide range of the parameters ϕ and μ.

4. At the equator the sum reduces to S of Eq. (A.15). A detailed discussion of the convergence of S is given in Appendix 3.

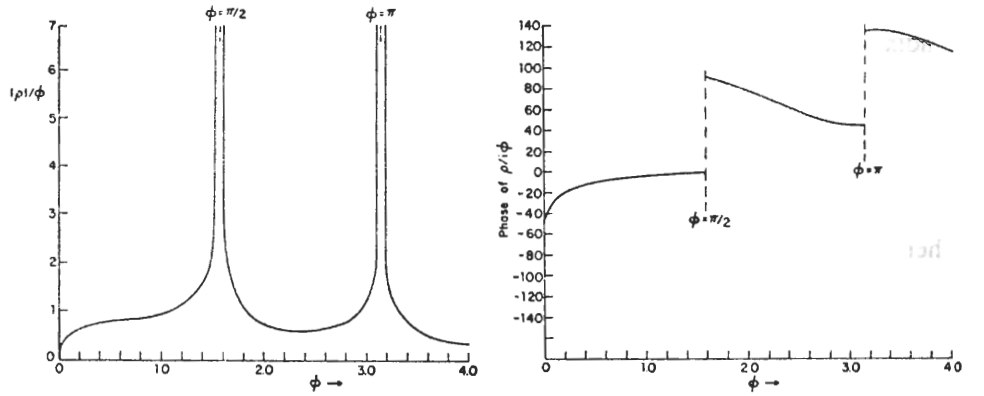

Figure 1. a) Amplitude of $\rho\,(i\phi)/i\phi$ for $\mu = .2$ (corresponding to a forcing scale of 10° of latitude) as a function of ϕ. x and y are scaled by $L_{eq} = (c/\beta)^{1/2}$.
b) Phase of $\rho\,(i\phi)/i\phi$ for $\mu = .2$ as a function of ϕ.

The function $\rho_N\,(i\phi)$ defined in eq. (20) becomes, in the analytic approximations accomplished in Appendix 3,

$$\rho\,(i\phi) \equiv Lim_{N \to \infty}\, \rho_N\,(i\phi)$$

$$= \left(\frac{\sqrt{1+\mu}}{(1-\mu^2)}\right) [i \sin 2\phi]^{-1/2} \left[\mu^{3/2} - \mu q\,(\mu, -\phi) + i \int_0^{\phi} q\,(\mu, -\phi')d\phi' \right] \qquad (23)$$

where

$$q\,(\mu, \phi) = [\mu \cos 2\phi - i \sin 2\phi]^{1/2}\,. \qquad (24)$$

Since, as we have pointed out in (22), the eastern boundary height response is given solely by $\rho\,(i\phi)$ and this function also sets the amplitude of the height response everywhere, we note some salient properties of this function.

For $\mu \equiv 0$ and ϕ small, $\rho\,(i\phi) = i\,2/3\,\phi$ so that

$$h_E = \frac{2}{3} X_E \exp\,[i\omega t]$$

so that the eastern boundary response is in phase with the wind everywhere equatorward of the turning latitudes when the wind has no meridional scale. When the wind does have a finite meridional scale $(2/\mu)^{1/2}$, for small ϕ,

$$\rho\,(i\phi) = -(1+\mu)^{1/2}\,(1-\mu^2)^{-1}\mu^{-1/2}\,(\phi/2)^{3/2} i^{-1/2}$$

so that

$$h_E = (1-\mu^2)^{-1}\,(8\mu)^{-1/2}\phi^{1/2} X_E \exp\left[i\omega t + \frac{\pi}{4} \right]$$

and the amplitude of the oscillations decreases as $\phi^{1/2}$ and the phase *leads* by $\pi/4$.

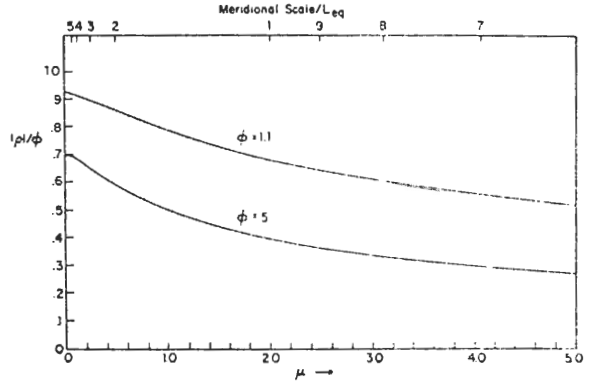

Figure 2. Amplitude of $\rho\,(i\phi)/i\phi$ as a function of μ for $\phi = .5$ and $\phi = 1.1$.

When both μ and ϕ are small but in such a way that $p = 2\phi\mu^{-1}$ is fixed,

$$\rho\,(i\phi) = (1+\mu)^{1/2}\,(2i\phi)^{-1/2}\mu^{3/2}\,(1-\mu^2)^{-1} \left[\, 1-(1+ip)^{1/2} + \frac{1}{3}\,[(1+ip)^{3/2}-1] \,\right] \tag{25}$$

so that

$$h_E = 2p^{-3/2}\left[\frac{2}{3} - (1+ip)^{1/2} + \frac{1}{3}(1+ip)^{3/2}\right] X_E \exp\left[\, i\omega t - \frac{3\pi}{4}\, i \,\right].$$

Figure 1 illustrates these behaviors by plotting the amplitude and phase of $\rho\,(i\phi)$ $(i\phi)^{-1}$ for $\mu = .2$. The resonances occurring when ϕ is a multiple of $\pi/2$ are readily apparent. The dependence of ρ on μ is illustrated in Figure 2 where the amplitude of $\rho\,(i\phi)\,(i\phi)^{-1}$ is plotted as a function of μ. The dependence is clearly weak for scales larger than 10° of latitude ($\mu<.2$), but the dependence is major for scales smaller than this.

The remainder of the manipulations leading to the analytic approximation to the general solution (19) is given in Appendix 3. The final result for response to the **symmetric forcing is:**

$$\begin{aligned}\mathbf{u} = (i\omega)^{-1}\exp[i\omega t]\Bigg\{ & \frac{1}{(1+\mu)^{1/2}}\,\frac{\rho\,(i\phi)}{t\,(0,\phi\xi)}\,\exp\left[\frac{y^2}{2}\,\eta\,(0,\phi\xi)\right]\begin{bmatrix} q^2\,(0,\phi\xi) \\ t^2\,(0,\phi\xi)\end{bmatrix} \\ & - \frac{\mu}{1-\mu^2}\exp\left[-\frac{1}{2}\,\mu y^2\right]\begin{bmatrix}\mu \\ 1\end{bmatrix} \\ & + \frac{\mu}{1-\mu^2}\,\frac{1}{t\,(\mu,\phi\xi)}\exp\left[\frac{1}{2}\,y^2\eta\,(\mu,\phi\xi)\right]\begin{bmatrix} q^2\,(\mu,\phi\xi) \\ t^2\,(\mu,\phi\xi)\end{bmatrix} \\ & + \frac{i}{1-\mu^2}\int_0^{\phi\xi} t^{-1}\,(\mu,\zeta)\exp\left[\frac{1}{2}\,y^2\eta\,(\mu,\zeta)\right]\begin{bmatrix} q^2\,(\mu,\zeta) \\ t^2\,(\mu,\zeta)\end{bmatrix} d\zeta \Bigg\}\end{aligned} \tag{26}$$

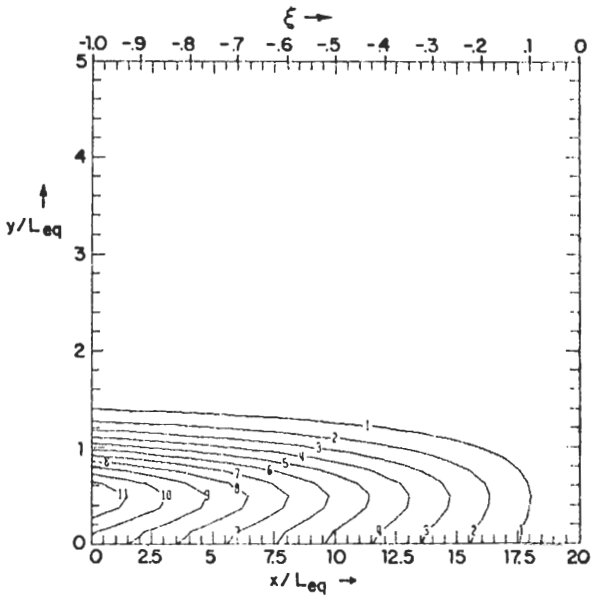

Figure 3. The low frequency (ϕ = .01) narrow symmetric forcing case (μ = 4.5, corresponding to a forcing scale of 3° of latitude).

a) Amplitude of height field oscillations normalized by X_B. Contour interval is .1.

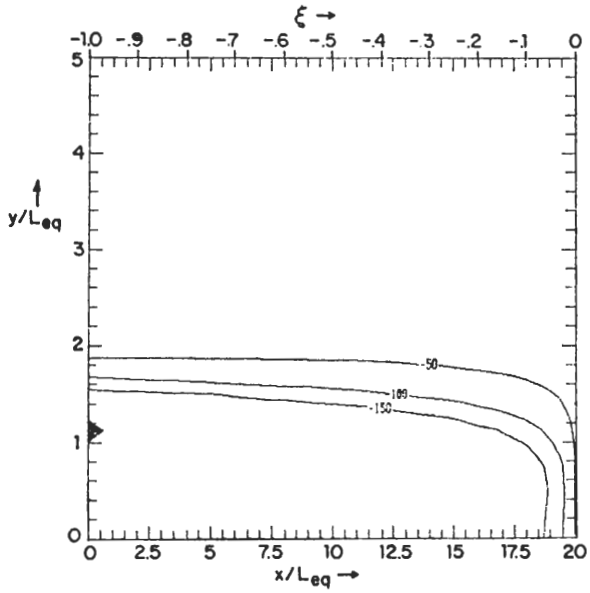

b) Phase of height field oscillation with respect to the forcing (negative phases *lead* the forcing). Contour interval 50°.

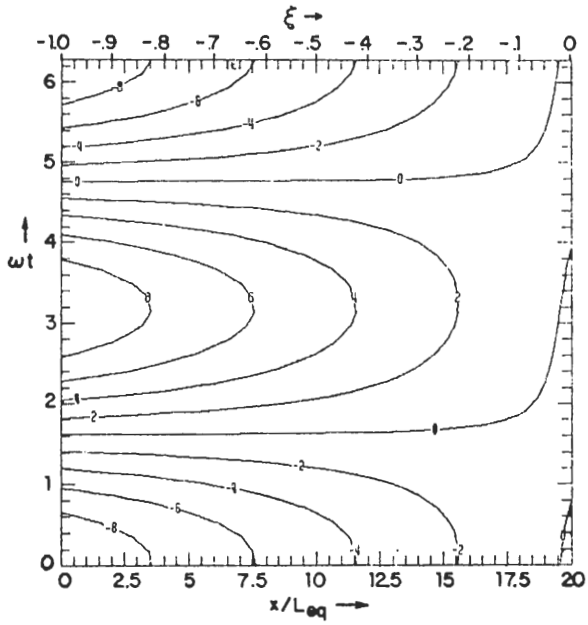

c) h/X_B *vs.* time on the equator. Contour interval .2. Time is scaled by ω^{-1}.

where q has already been defined in (24),

$$t(\mu, \phi) = [\cos 2\phi - \mu i \sin 2\phi]^{1/2}, \tag{27}$$

and

$$\eta(\mu, \phi) = -\frac{q^2(\mu, \phi)}{t^2(\mu, \phi)} = \frac{i(1-\mu^2)\tan 2\phi - \mu \sec^2 2\phi}{1 + \mu^2 \tan^2 2\phi}. \tag{28}$$

We note immediately that $t(\mu, 0) = 1$, $q(\mu, 0) = \mu^{1/2}$ and that $\eta(\mu, 0) = -\mu$ so that at the eastern boundary of the basin ($\xi = 0$), $u = 0$, and h_E reduces to (22). We also note that u is singular when $2\phi\xi$ is an odd multiple of $\pi/2$ while h is well behaved—we will discuss these points ("foci" in the ray theory language of Schopf, Anderson and Smith, 1981), in detail below.

We proceed to examine the solution (19) and its analytic approximation (26) over the range of the parameters ϕ and μ. We emphasize that all figures presented in the discussion are drawn by means of the mode summation given in (19)—the analytic form (26) will be used to explain the features shown therein.

a. The small ϕ case.

The first case of interest is $\phi << 1$, a case that corresponds either to extremely long periods or very small basins or both. For orientation, a baroclinic mode with equivalent depth 60 cm (Kelvin wave speed 2.5 m sec^{-1}) in a basin 5000 km long

would produce a ϕ of .1 for an oscillation period of five years; longer periodicities, of course, produce smaller values of ϕ.

Figure 3 shows the amplitude (Fig. 3a) and phase (Fig. 3b) of the height field response for $\phi = .01$ and $\mu = 4.5$. (This value of μ corresponds to a zonal forcing tightly confined to the equator with half width 300 km.) The analytic form (26) for $\phi << 1$ and for $y^2 << \phi^{-1}$ reduces to

$$h = X_E \exp[i\omega t] \left\{ (i\phi)^{-1} (1+\mu)^{-1/2} \rho(i\phi) + \xi (1+\mu y^2) \exp\left[-\frac{1}{2} \mu y^2 \right] \right\} . \tag{29}$$

We note immediately that (29) is consistent with the steady "Sverdrup" solution $h_x = F - yF_y$ (Cane and Sarachik, 1977; Eq. (25c)) so that the tilt of the height field is in phase with the forcing everywhere. This does not, however, imply that the height field itself is in equilibrium with the forcing since integration of the steady solution in x yields $h/X_E = h_E/X_E + \xi (F - yF_y)$ which is identical to (29). However, since h_E is proportional to ρ (Eq. (22)) and ρ is complex, there will be a phase variation of the height field response with respect to the forcing as we move across the basin: equilibrium of the height field *tilt* does not therefore insure equilibrium of the height field in this symmetric forcing case. We will confine the usage of the term "equilibrium" to the more restrictive case where the height field is in equilibrium with the forcing.

We see that far above the half-width of the forcing the height field oscillation asymptotes to

$$h \to X_E \exp[i\omega t] (i\phi)^{-1} (1+\mu)^{-1/2} \rho(i\phi) \approx \frac{1}{2} p^{1/2} X_E \exp[i\omega t + \pi/4] \tag{30}$$

since in this case, $p = 4.44 \times 10^{-3}$ is small. Even far above the forcing region, the amplitude of the oscillation is $p^{1/2}/2 = 3.3 \times 10^{-2}$ and the response *leads* the forcing by $\pi/4$. At the eastern boundary, equatorward of the turning points, the response is also given by (30).

On the equator

$$h(y=0) = \left(\frac{1}{2} p^{1/2} \exp[i\pi/4] + \xi \right) X_E \exp[i\omega t] \tag{31}$$

so that, on the equator, the amplitude of the height field oscillation is $\{[(p/8)^{1/2} + \xi]^2 + p/8\}^{1/2}$ and ranges from $2^{-1}p^{1/2}$ at the eastern boundary to $1\text{-}2^{-1}p^{1/2}$ at the west. Similarly, on the equator, the phase is given by arc tan $[-(2\xi + p^{1/2})^{-1}p^{1/2}]$ and ranges from $-\pi/4$ at the eastern boundary to $-\pi + 2^{-1}p^{1/2}$ at the west, with most of the transition taking place in a region of width $0(p^{1/2})$ in ξ from the eastern boundary. These features, on the equator, are better illustrated in a time-height diagram, Figure 3c.

Off the equator, the amplitude is

$$A = \left\{ [(p/8)^{1/2} + \xi\,(1 + \mu y^2)\exp[-1/2\,\mu y^2]]^2 + p/8 \right\}^{1/2} \tag{32}$$

and has a maximum at $y = \mu^{-1/2}$ independent of ξ except within a region of order $p^{1/2}$ of the eastern boundary. For the parameter $\mu = 4.5$ of Figure 3a, this maximum occurs at $y = .47$. The amplitude increases westward and attains its maximum value at $\xi = -1$, $y = .47$: its value at this point is 1.19 obtained directly from (32). Finally, off the equator, we may compare the phase in Figure 3b with the analytic expression

$$\phi = -\arctan\left\{ (p/8)^{1/2}\left[(p/8)^{1/2} + \xi\,(1 + \mu y^2)\exp\left[-\frac{1}{2}\mu y^2 \right]\right]^{-1} \right\}.$$

Since this phase is relatively featureless beyond those aspects we have already explained, let us simply note that this analytic expression for the phase precisely describes the detailed behavior of the phase illustrated in Figure 3b.

Figure 4 illustrates a case for ϕ small ($= .01$) but now with the meridional scale wide enough ($\mu = .006$ corresponding to a half-width of about 60° of latitude for the first baroclinic mode) so that $p = 2\phi/\mu$ is no longer small; $p = 3.133$. Since ϕ is so small, (29) still holds. It should be noted that since the diagrams in Figures 4a and 4b are confined to five equatorial radii of deformation of the equator, very little y dependence is visible. The evaluation of ρ for this case using (25) yields the height field

$$h = X_E \exp[i\omega t]\left\{ .592\exp[.266i] + \xi\,(1 + \mu y^2)\exp[-1/2\,\mu y^2] \right\}. \tag{33}$$

If we ignore the barely perceptible y dependence the amplitude becomes $[(.572 + \xi)^2 + (.156)^2]^{1/2}$ and the phase becomes $\chi = -\arctan[.156(.572 + \xi)^{-1}]$. Thus the value of the amplitude minimum is .156 and the phase passes through −90° at the minimum. The phase ranges from −15° (leads) at the eastern boundary to about −160° at the western with slow variation across the basin. To get some feel for reading amplitude and phase diagrams when the amplitude has a minimum, we have included a time-height slice across the equator. We clearly see the minimum amplitude point at $\xi = -.572$. That the phase leads by 90° at this point means that the oscillation reaches zero (halfway between the maximum at +.156 on its way to the minimum at −.156) when the forcing is still at its maximum (say at $t = 0$). That the phase varies across the basin simply indicates that the height field oscillation is not taking place about the point $\xi = .572$ as a rigid seesaw about the pivot but rather as a writhing snake. To the extent that the phase variation is slow, we can define a local wave number $\partial\chi/\partial x$ where we recall that the phase is defined by

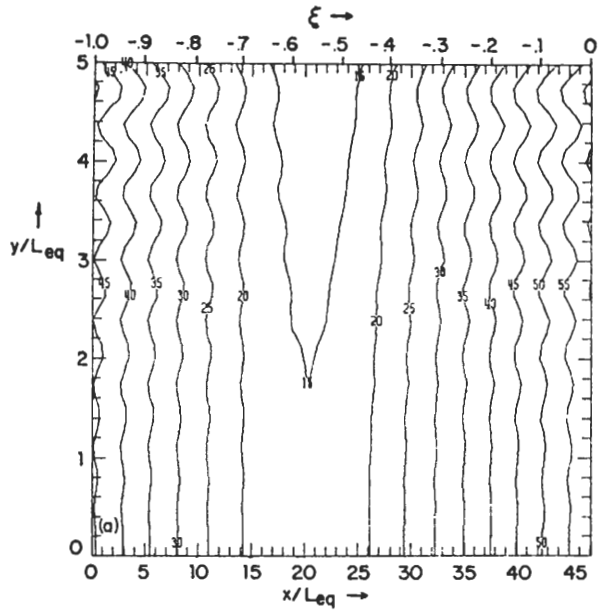

Figure 4. The low frequency (ϕ = .01) wide symmetric forcing case (μ = .006, corresponding to a forcing side of 60° of latitude).

a) Amplitude of h/X_B. Contour interval is .05.

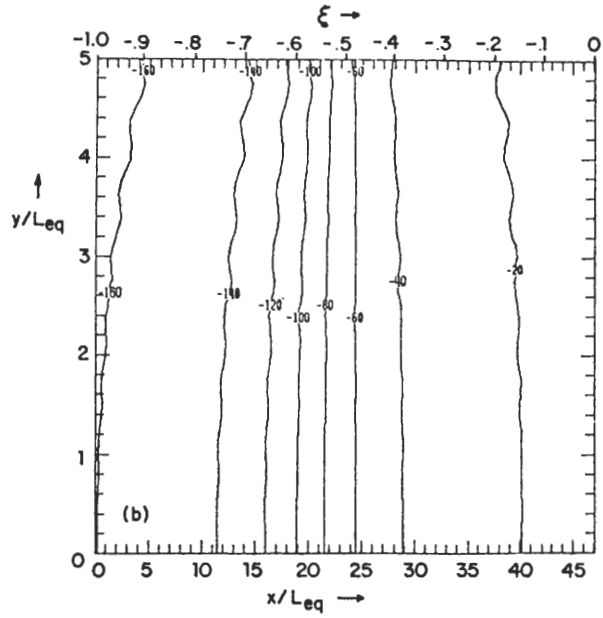

b) Phase of h with respect to forcing (negative phases lead). Contour interval 20°.

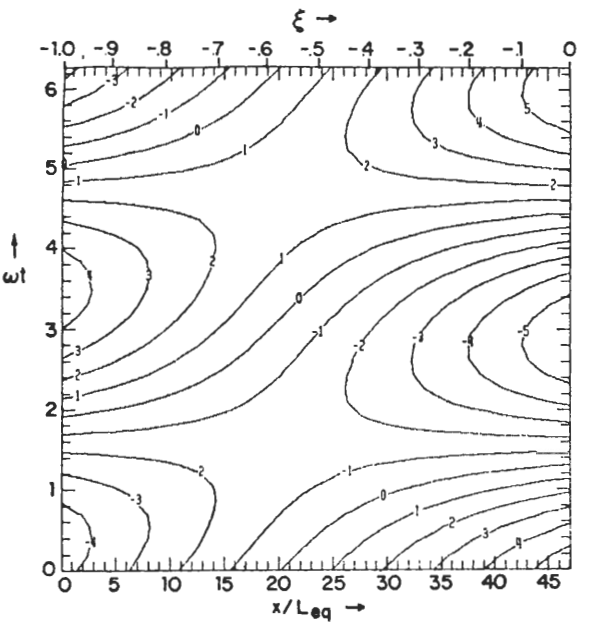

c) h/X_B *vs.* time on the equator. Contour interval .1.

$h = |h| \exp[-i\chi]$. In terms of the local wavenumber there would be a zonal phase propagation speed $c_{\text{phase}} = \omega/(\partial\chi)/\partial x$ which, since the phase is increasing eastward, would imply an *eastward* phase propagation. We thus have the circumstance that a few radii of deformation away from the equator, where the Kelvin wave amplitude is surely negligible and only westward propagating Rossby waves exist, the phase propagation is eastward. Since the essence of the problem involves waves oscillating at a single frequency, it should not be surprising that the *sum* of such oscillations can lead to interfering phase patterns having little relation to the individual waves comprising the sum. No phase propagation characteristic of an "annual Rossby wave" is seen in the sum nor in general should any be expected.

When the forcing is so wide that $p >> 1$ (still for $\phi << 1$), then the height field variations are simply given by

$$h = \left(\frac{2}{3} + \xi\right) X_E \exp[i\omega t] \tag{34}$$

for all y. Here the height field *is* oscillating like a rigid seesaw in phase with the wind to the east of the pivot point $\xi = -2/3$ and out of phase with the wind to the west of this point: this is the limit that corresponds to "equilibrium." This limit has usually been attributed to low frequency (or small basin) only (e.g., Philander, 1979) but as we see here the forcing must also be wide enough so that p is large. As we will see below, some not so small ϕ cases will exhibit approximate equilib-

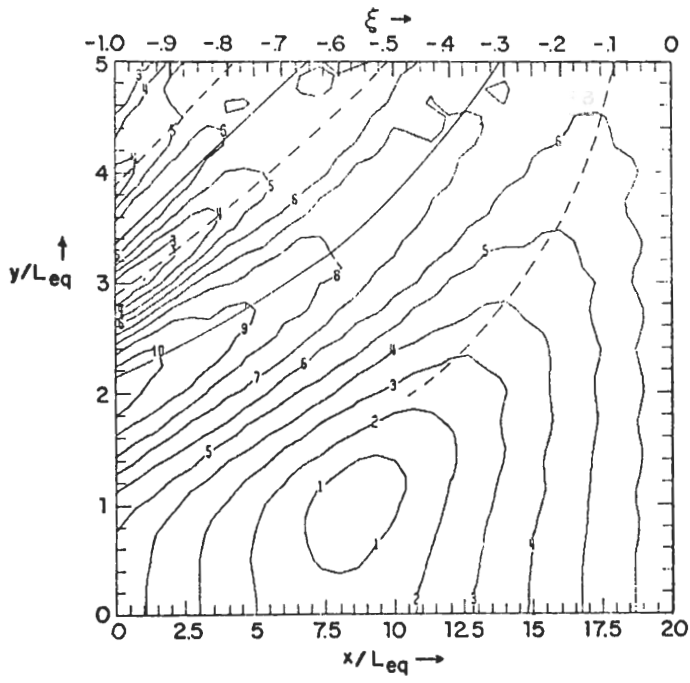

Figure 5. The Atlantic Annual ($\phi = .54$) Symmetric Forcing Case ($\mu = .2$, corresponding to a forcing scale of 10° of latitude).

a) Amplitude of h/X_E. Contour interval .1. Dashed lines indicate minima and solid lines maxima of oscillation amplitudes according to (39).

rium response on the equator but almost nowhere else and so will not correspond to an equilibrium response. As a final point we may note that in the limit $\omega \to 0$, $h \to (2/3 + \xi)X_E$. This may seem strange, since in the steady case of $F = 1$, the height field will balance the wind stress in Eq. (1) with $h = (1/2 + \xi)X_E$ if mass is conserved. The point here, of course, is that in a meridionally infinite β-plane, mass need not be conserved since there will be interchange with the reservoir at infinity. The imposition of boundaries at the north and the south (using the methods of Cane and Sarachik, 1979) will change the pivot from $\xi = -2/3$ to $\xi = -1/2$ since mass *will* be conserved in the closed basin case.

b. The $\phi = 0$ (1) case.

When ϕ is no longer small compared to unity, a glance at Figure 6 shows that some new and interesting features occur. In particular, when $\phi > \pi/4$ there will be at least one value of ξ for which $2\phi\xi = -\pi/2$. At such a point (a "focus"), the analytic result (26) indicates that u is singular, h has small amplitude and the phase

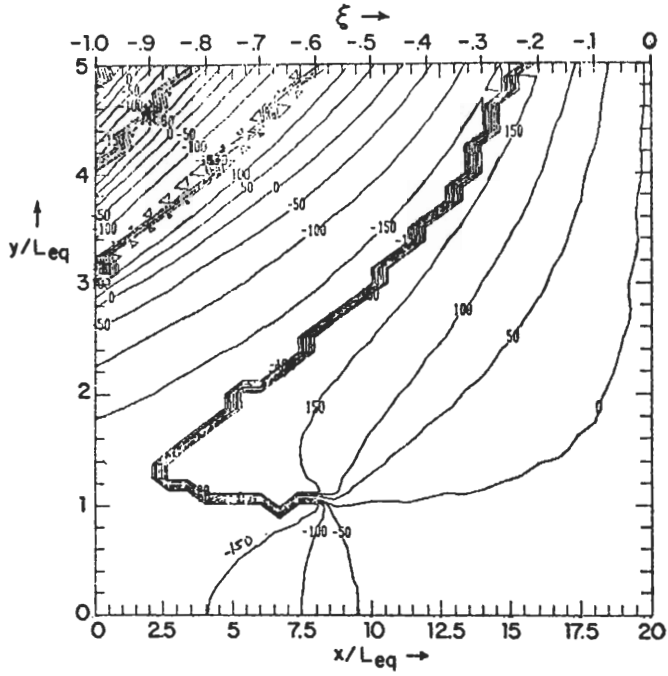

b) Phase of h with respect to forcing (negative phases lead the forcing). Thick multiple lines are the contour package's way of going from 180° to −180° so have no special significance. Contour interval 50°.

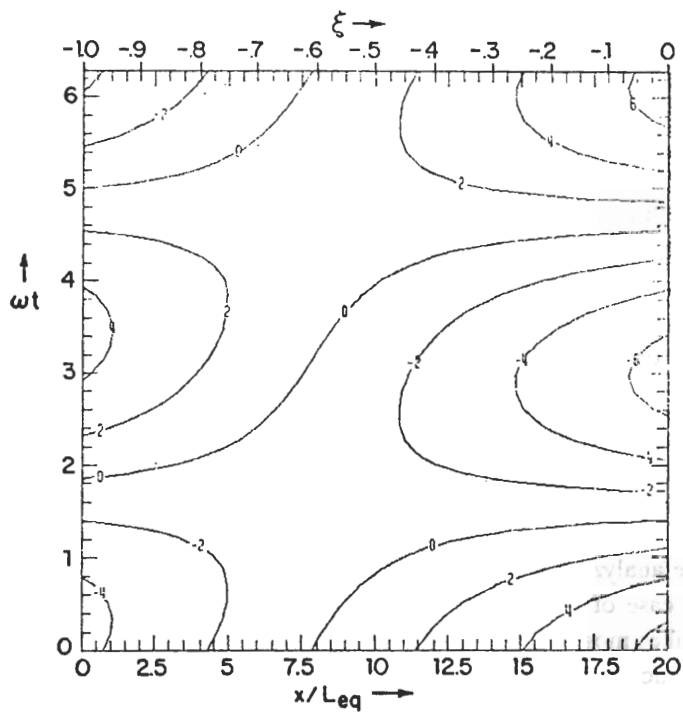

c) h/X_R *vs.* time on the equator. Contour interval .2.

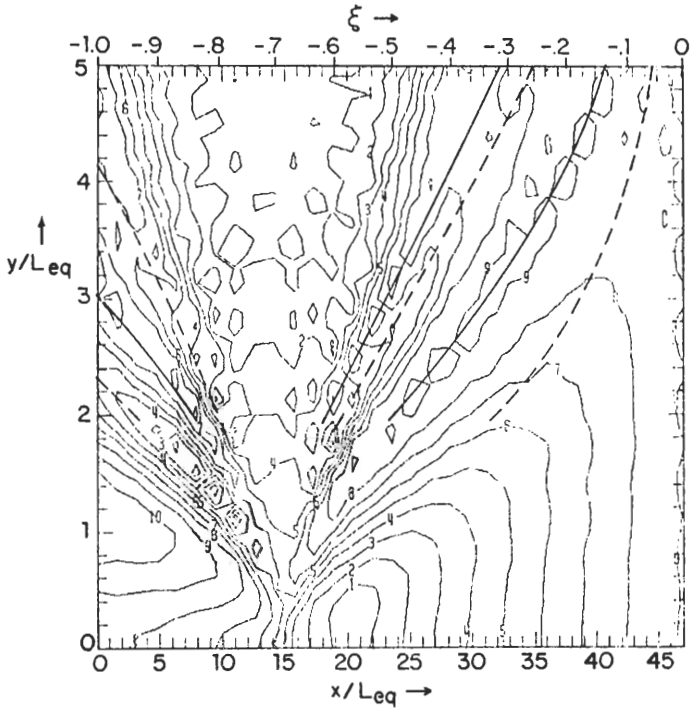

Figure 6. The Pacific Annual (ϕ = 1.13) Symmetric Forcing Case (μ = .2, corresponding to forcing scale of 10° of latitude).
a) Amplitude of h/X_R. Contour interval .1. Dashed lines indicate minima and solid lines maxima of oscillation amplitudes according to (39).

variation of both u and h becomes very rapid in a parabolic zone ("shadow zone") expanding poleward away from the equator. This zone is bounded by large amplitude regions ("caustics") extending northeastward and northwestward from the focus. The words in quotes are the ray descriptions of these features, first given by Schopf, Anderson and Smith (1981) for the equatorial problem. They, however, did not solve a forced problem and derived only very general kinematic properties of periodic Rossby rays. As we will see in the remainder of this section, the situation for the forced problem is somewhat more complicated than that indicated by Schopf *et al.* (1981).

The difficulty in interpreting (26) arises from the integral term. In general, the integral can be analyzed for large y^2 by using the method of steepest descent but in the particular case of $\mu = 0$ we can give a particularly simple analysis that qualitatively describes most of the features of the $\phi = 0$ (1) case and, in addition, has a good degree of accuracy for μ less than unity, and y greater than unity.

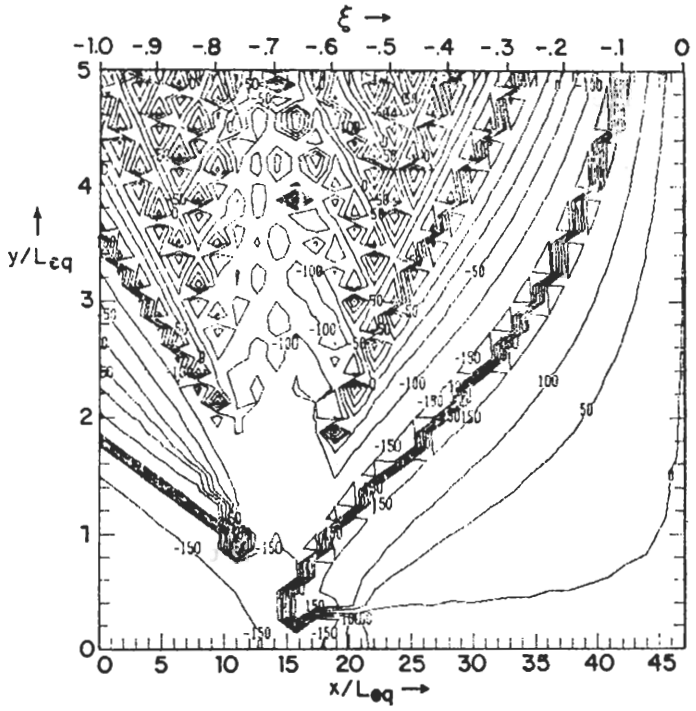

b) Phase of h with respect to the forcing (negative phases lead). Contour interval is 50°.

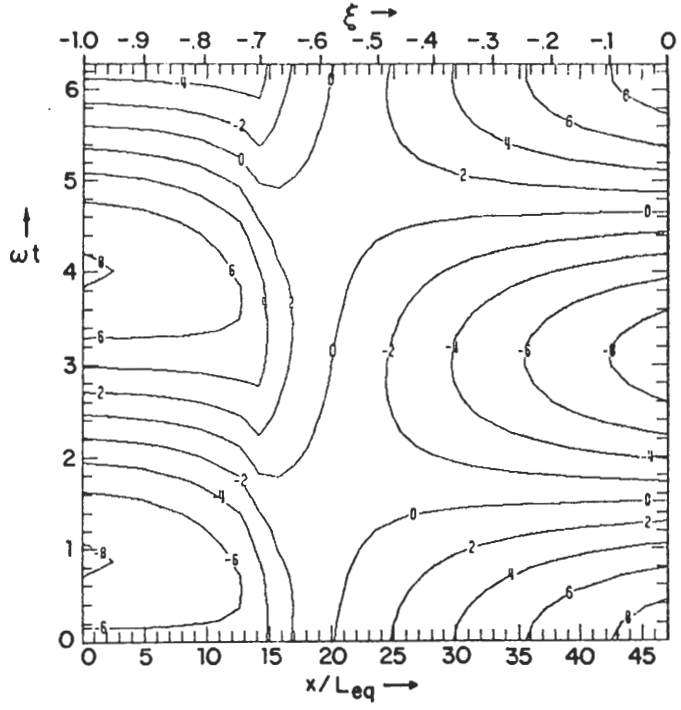

c) h/X_B *vs.* time on the equator. Contour interval is .2.

In order to confine ourselves to the cases illustrated in Figures 6 and 7, we will choose $\phi < \pi/2$. The height field in this $\mu = 0$ case then becomes[5]

$$h/X_E = \phi^{-1} \left\{ \rho_0 \exp\left[i \frac{y^2}{2} \tan 2\phi\xi \right] (\cos 2\phi\xi)^{1/2} + \int_0^{\phi\xi} \exp\left[i \frac{1}{2} y^2 \tan 2\zeta \right] (\cos 2\zeta)^{1/2} d\zeta \right\} \exp[i\omega t] \tag{35}$$

where ρ_0 is the real (for $\phi < \pi/2$) number

$$\rho_0 = (\sin 2\phi)^{-1/2} \int_0^{\phi} (\sin 2\phi')^{1/2}\, d\phi' \ .$$

The integral term in (35) vanishes for large y^2 by the generalized Riemann-Lebesgue Lemma (Bender and Orszag, 1978, Sec. 6.5), since the tangent in the exponent is continuously differentiable. The integral can in fact be asymptotically expanded in inverse powers of y^2 simply by a series of partial integrations. We will content ourselves with a single partial integration to write the height field, neglecting terms of $0(1/y^4)$ as

$$h/X_E = \phi^{-1} \left\{ \rho_0 \exp\left[i \frac{1}{2} y^2 \tan 2\phi\xi \right] (\cos 2\phi\xi)^{1/2} + (iy^2)^{-1} \left[(\cos 2\phi\xi)^{5/2} \exp\left[i \frac{1}{2} y^2 \tan 2\phi\xi \right] - 1 \right] \right\} \exp([i\omega t] \ . \tag{36}$$

In terms of the auxiliary phase function

$$\psi = \frac{1}{2} y^2 \tan 2\phi\xi - (\rho_0 y^2)^{-1} (\cos 2\phi\xi)^2$$

we can then easily explicitly derive the amplitude $|h|$ and phase, $-\chi$, of the height field variations for large y.

For $-\pi\,(4\phi)^{-1} < \xi \leqslant 0$,

$$|h|/X_E = \phi^{-1} \left\{ \rho^2{}_0 \cos 2\phi\xi + 2y^{-2}\rho_0 \sin\psi\, (\cos 2\phi\xi)^{1/2} + 0\,(y^{-4}) \right\}^{1/2} \tag{37a}$$

and

$$\tan\chi = -\tan\psi - (y^2\rho_0 \cos\psi)^{-1} (\cos 2\phi\xi)^{-1/2} \ . \tag{37b}$$

5. Strictly speaking, the $\mu = 0$ approximation breaks down for the integral in the shadow zone (see the discussion in Section 5) but since the first term of (35) dominates in the shadow zone, (35) and (36) give good asymptotic approximations everywhere.

For $-1 < \xi < -\pi\,(4\phi)^{-1}$,

$$|h|/X_E = \phi^{-1}\left\{ -\rho_0^2 \cos 2\phi\xi + 2y^{-2}\rho_0 \cos\psi\,(-\cos 2\phi\xi)^{1/2} + 0\,(y^{-4}) \right\}^{1/2} \tag{38a}$$

and

$$\tan\chi = \cot\psi + (y^2\rho_0 \sin\psi)^{-1}\,(-\cos 2\phi\xi)^{-1/2}\,. \tag{38b}$$

It is easily seen from (37a) and (37b) that the amplitude has extrema when

$$2\sin\psi - \rho_0 \sin 4\phi\xi\,(\cos 2\phi\xi)^{1/2} - y^{-2}\sin 4\phi\xi \sin\psi = 0 \tag{39a}$$

or

$$2\sin\psi + \rho_0 \sin 4\phi\xi\,(-\cos 2\phi\xi)^{1/2} + y^{-2}\sin 4\phi\xi\cos\psi = 0 \tag{39b}$$

east or west of the focus at $\xi = -\pi\,(4\phi)^{-1}$, respectively. Figures 5a and 6a show the locations of the maxima and minima given by (39) drawn in for $y > 2$. In the shadow zone between the two large maxima in Figure 6a, the amplitude becomes highly oscillatory and small.

The lines of constant phase are given by (37b) and (38b) and it can be verified that these reproduce the phase lines in Figures 5b and 6b for $y \gtrsim 2$. In fact, for y^2 large, the phase becomes, to a very good approximation,

$$\chi = -\frac{y^2}{2}\tan 2\phi\xi + 0\,(y^{-2}) \tag{40}$$

which itself illustrates most of the features of Figures 5b and 6b for $y \gtrsim 2$. In particular, the phase given by (40) shows the characteristic parabolic pattern radiating out from the focus and shows rapid oscillation as the focus $\xi = -\pi\,(4\phi)^{-1}$ is approached, the zone of rapid oscillation expanding northward with the lines of constant phase in Figure 6b. Near the eastern boundary, $\xi = 0$, (40) fails but it is easily seen from (37b) that $\chi \sim -(\rho_0 y^2)^{-1}$ so that the phase leads slightly on the eastern boundary, the lead approaching zero as y^2 increases as is illustrated in both Figures 5b and 6b.

As long as μ is small compared to unity, the $\mu = 0$ analysis presented above works quite well, quantitatively as well as qualitatively for both the amplitude and the phase, if y is large ($y = 2$ seems to be large enough). The amplitude also proves to be relatively independent of the precise value of μ as long as μ is small—an amplitude diagram generated for $\mu = .006$ proved to be almost indistinguishable from Figure 6a (this is also consistent with the weak μ dependence of ρ in Figure 2, for small μ).

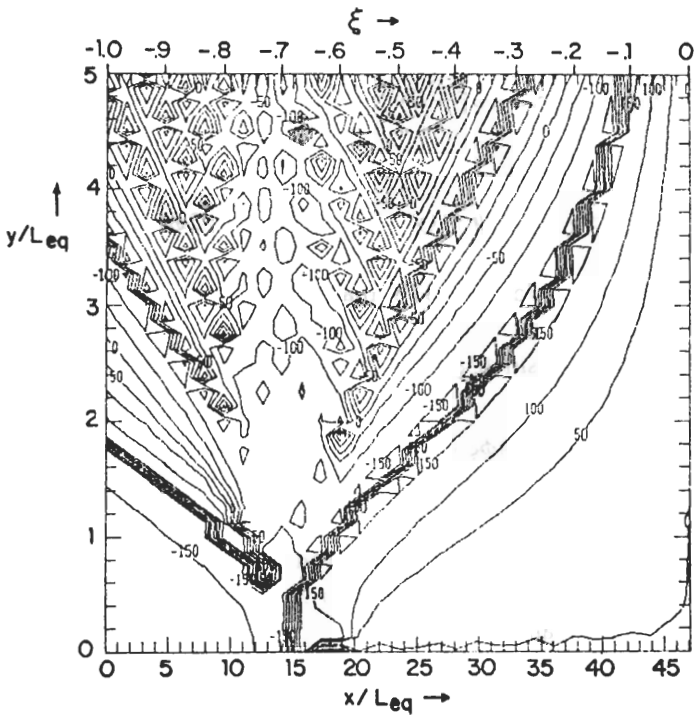

Figure 7. Phase of h for Pacific Annual ($\phi = 1.13$) Symmetric Forcing Case but for wide forcing ($\mu = .006$, corresponding to a scale of 60° of latitude). Contour interval 50°.

The *phase* behavior for small μ, however, *does* depend on the precise value of μ, but only within one or two radii of deformation of the equator. Consideration of (35) on the equator shows that, for $\mu = 0$, h is in phase with the forcing to the east of the focus and gradually acquires a non-zero phase as we move to the west of the focus. Figure 7 shows this behavior for $\mu = .006$ and we may conclude that to the east of the focus the smaller the value of μ, the closer is the zero phase line to the equator. As μ increases from zero, the zero phase line moves off the equator and equatorward of the zero phase line, the phase *leads* with the lead increasing westward. To the extent that the phase varies slowly enough, we can use the argument given previously to conclude that equatorward of the zero phase line, the apparent phase propagation will be eastward while poleward of the zero phase line it will be westward.

In both Figures 5b and 6b, the phase near the equator leads by something near zero at the east and something near 180° at the west. The effective wavenumber therefore is of order π/X_E. The eastward phase propagation speed is then $\omega\pi/X_E$

$\cong 2X_E/T$ where T is the period of the forcing. For annual forcing in a basin 5000 km long, the eastward phase propagation speed is π^{-1} m/sec.[6] We may note that an eastward phase propagation speed of 30 cm/sec for the seasonal thermocline response along the equator in the Atlantic has recently been noted by Merle (1980).

5. Response to an anti-symmetric zonal forcing

The general solution for the periodic response to a zonal forcing anti-symmetric about the equator can be read off directly from (19) by simply noting that no Kelvin wave can be excited:

$$\mathbf{u} = (i\omega)^{-1} \exp[i\omega t] \left\{ \sum_{n=0}^{N} r_{2n}\mathbf{R}_{2n} [1 - \exp[i\phi\xi (4n+1)]] \right\} . \tag{41}$$

We see immediately that the height field h as well as the zonal velocity u vanishes at the eastern boundary, for, as we have noted in the discussion following (22), it is the term involving the Kelvin wave plus its reflections which set the magnitude and phase of the height field oscillations at the eastern boundary. Alternately, we may note that the height field oscillates with uniform magnitude equatorward of the turning points and since the magnitude at the equator vanishes by anti-symmetry, it must vanish everywhere along the eastern boundary.

As in the symmetric case, we can examine a wide range of properties of the response to anti-symmetric forcing by choosing the idealized form $F = y \exp[-1/2\ \mu y^2]$ for which an approximate analytic solution may be obtained. This particular forcing has its maximum at $y = \mu^{-1/2}$, its value at the maximum being $(\mu e)^{-1/2}$.

The sum can again be extended to $N \to \infty$ using the same approximation as before and analytically summed (the details are given in Appendix 3) with the final result:

$$\mathbf{u}/X_E = \frac{\mu y}{1-\mu^2} \left\{ t^{-3}(\mu,\phi\xi) \exp\left[\frac{1}{2} y^2\eta(\mu,\phi\xi)\right] \begin{bmatrix} q^2(\mu,\phi\xi) \\ t^2(\mu,\phi\xi) \end{bmatrix} - \exp\left[-\frac{1}{2}\mu y^2\right] \begin{bmatrix} \mu \\ 1 \end{bmatrix} \right.$$
$$\left. - i \int_0^{\phi\xi} t^{-3}(\mu,\zeta) \exp\left[\frac{1}{2} y^2\eta(\mu,\zeta)\right] \begin{bmatrix} t^2(\mu,\zeta) \\ q^2(\mu,\zeta) \end{bmatrix} d\zeta \right\} \frac{\exp[i\omega t]}{i\phi} . \tag{42}$$

6. The factor of π arises because the year has $\pi \times 10^7$ sec.

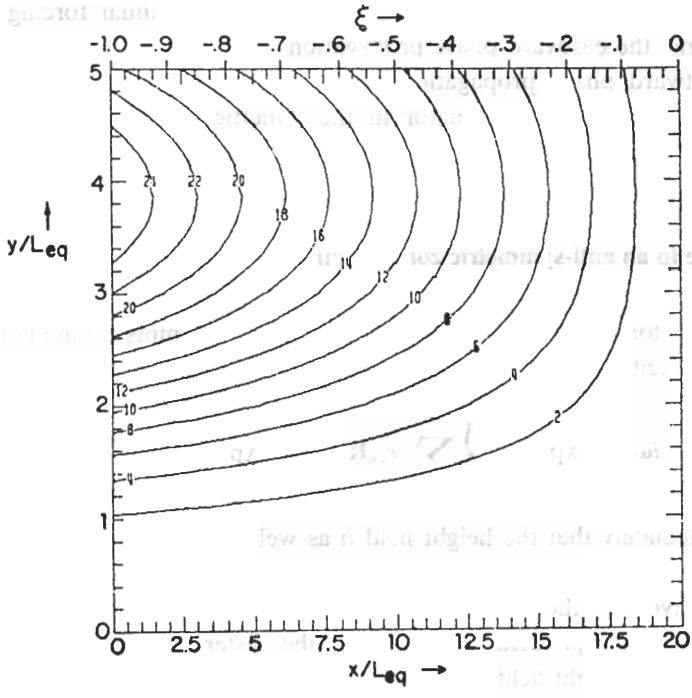

Figure 8. The low frequency (ϕ = .01) Anti-Symmetric Case with μ = .02 amplitude of h/X_E. Contour interval .2. (Phase is uniform across basin so is not shown—see text.)

The functions $q\,(\mu,\phi)$, $t\,(\mu,\phi)$ and $\eta\,(\mu,\phi)$ have been previously defined by (24), (27) and (28), respectively.

a. The small ϕ case.

In the limit that $\phi << 1$ and for $y^2 << \phi^{-1}$, the solution (42) for the height field reduces simply to

$$h/X_E = \mu\xi y^3 \exp\left[-\frac{1}{2}\mu y^2 \right] \exp\left[i\omega t\right] . \tag{43}$$

Again we may note that this is equivalent to the low frequency "Sverdrup" limit $h_x = F - yF_y$ given in Cane and Sarachik (1977), Eq. (25c). We also note that the response is 180° out of phase (since $\xi < 0$) with the forcing with no phase variation across the basin, either zonally or meridionally.

Figure 8 shows the solution, obtained by summing modes, for $\mu = .2$ and $\phi = .01$; it is almost identical (to $0(\phi)$) with the analytic solution (42). In particular, the amplitude increases westward as $|\xi|$ and has a maximum at $y = (3/\mu)^{+1/2}$ (3.87 for the parameters of Fig. 8). The phase (not shown) was verified to be within $0(\phi)$ of 180° everywhere.

b. The $\phi \sim 0(1)$ case.

As in the symmetric case, the general solution (41) has the integral term which is not easily interpretable. We can gain a qualitative understanding of what is going on in this case by considering the shadow zone and the region exterior to the shadow zone separately. If we consider μ small, the region for which $\mu y^2 \sec^2 2\phi\xi$ is small may be taken as a definition of the region outside the shadow zone. In this case the integral in (42) may be partially integrated as before to give the asymptotic result, outside the shadow zone,

$$h/X_E \sim \mu y \left\{ (\cos 2\phi\xi)^{-1/2} \left[\exp\left[-\frac{1}{2}\mu y^2 \sec^2 2\phi\xi \right] + i(2y^2)^{-1} \sin 4\phi\xi \exp\left[\frac{1}{2} iy^2 \tan 2\phi\xi \right] \right] - \exp\left[-\frac{1}{2}\mu y^2 \right] \right\} (i\phi)^{-1} \exp[i\omega t] \,. \tag{44}$$

As long as $\phi < \pi/4$, so that there will be no focus and no shadow zone, (44) provides a reasonable asymptotic approximation for $y \geqslant 2$. Figure 9 shows the amplitude and phase of the height field oscillations for parameters characteristic of anti-symmetric zonal forcing with $\mu = .2$ in the Atlantic; $\phi = .54 < \pi/4$. Superimposed on the amplitude diagram are the lines of relative maxima and minima given directly by Eq. (44)—we see that the qualitative behavior of the pattern is reproduced, for $y \geqslant 2$, by this asymptotic result. By plotting (44) directly for this case, we have verified that the asymptotic approximation is accurate to 10% for $y \geqslant 2$ when compared to the modal sums, the accuracy improving with increasing distance from the equator.

When $\phi \geqslant \pi/4$, the characteristic focus-caustic-shadow zone structure exists also in the anti-symmetric forcing case, the focus again being at $\phi\xi = -\pi/4$. Figure 10 shows the response to anti-symmetric forcing with $\mu = .2$ for parameters characteristic of annual forcing in the Pacific, $\phi = 1.13$. Since $\mu y^2 \sec^2 2\phi\xi$ is no longer small as the focus is approached, the approximation given by (44) breaks down: it only holds in the regions where $\mu y^2 \sec^2 2\phi\xi$ *is* small, namely, outside the shadow zone. The integral is asymptotically approximated, by partial integration, as

$$I = -\int_0^{\phi\xi} \sin 2\zeta (\cos 2\zeta)^{-3/2} \exp\left[-\frac{1}{2}\mu y^2 \sec^2 2\zeta \right] \exp\left[i\frac{y^2}{2} \tan 2\zeta \right] d\zeta$$
$$\approx -(iy^2)^{-1} (\cos 2\phi\xi_0)^{1/2} \sin 2\phi\xi_0 \exp\left[i\frac{y^2}{2} \tan 2\phi\xi_0 \right] \tag{45}$$

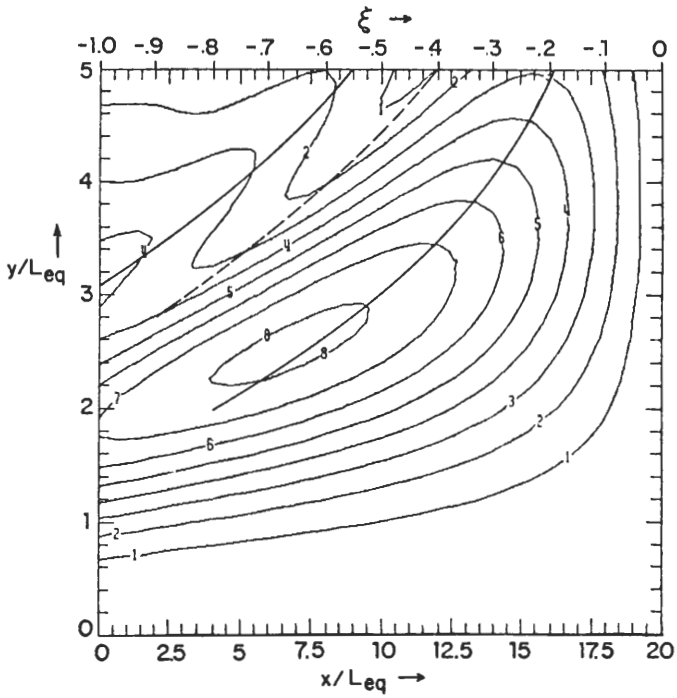

Figure 9. The Atlantic Annual ($\phi = .54$) Anti-Symmetric Forcing Case for $\mu = .2$.
a) Amplitude of h/X_E. Contour interval is .1. Solid lines indicate maxima and dashed line minima according to (44).

where ξ_0 is defined arbitrarily by

$$\frac{1}{2}\mu y^2 \sec^2 2\phi\xi_0 = C << 1 \tag{46}$$

and C is some small constant. The essence of the approximation (45) is that there will no longer be any contribution to the integral for $|\phi\xi| > |\phi\xi_0|$ since the exp $[-1/2\ \mu y^2 \sec^2 2\zeta]$ is so small. If y^2 is so large that (46) can no longer be satisfied, it is clear that the integral now vanishes exponentially and

$$h/X_E \sim i\mu y\phi^{-1} \exp\left[-\frac{1}{2}\mu y^2\right] \exp[i\omega t]\ . \tag{47}$$

Inside the shadow zone, (47) is also an excellent approximation and we see that the amplitude becomes smooth, independent of ξ, and the phase leads the forcing by $\pi/2$, again independent of ξ, as illustrated in Figure 10. In Figure 10a, the relative maxima and minima given by the approximation (44) applied outside the shadow zone are shown while it is clear from both Figures 10a and 10b that (47) applies inside the shadow zone.

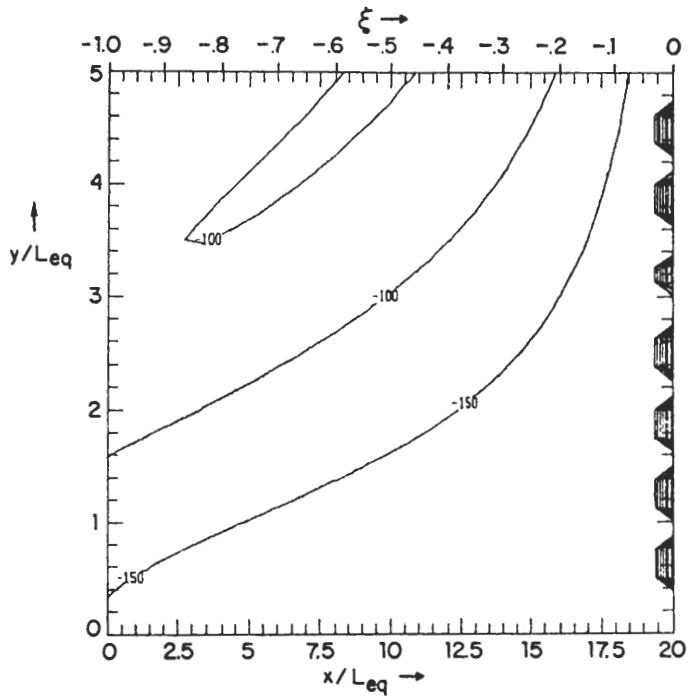

b) Phase of h with respect to the forcing (negative phases lead). Contour interval 50°. Hash on eastern boundary occurs where amplitude is zero so has no significance.

In both Figure 9b and Figure 10b we see that the phase decreases eastward and so corresponds to a westward zonal phase velocity. Since there is hardly any phase variation in the shadow zone in Figure 10b, the zonal phase velocity there would be effectively zero.

6. Conclusion

In this paper we have examined the periodic response of the linear inviscid shallow water equations in a meridionally unbounded basin to zonal forcings at a single low frequency ω. A general solution in the long wave approximation and on an equatorial β-plane was obtained by summing the Kelvin mode and the finite sum of Rossby modes whose turning points lie equatorward of the turning latitude at frequency ω. The character of the response was shown to depend on the parameter $\phi = \omega X_E$ where X_E is the zonal extent of the basin. (In terms of dimensional variables $\phi = \omega X_E/c$ where c is the speed of the Kelvin wave.) For the simplest symmetric zonal forcing $\exp[-1/2\mu y^2 + i\omega t]$ and the simplest anti-symmetric zonal forcing $y \exp[-1/2\mu y^2 + i\omega t]$, the sum was extended to infinity and performed analytically.

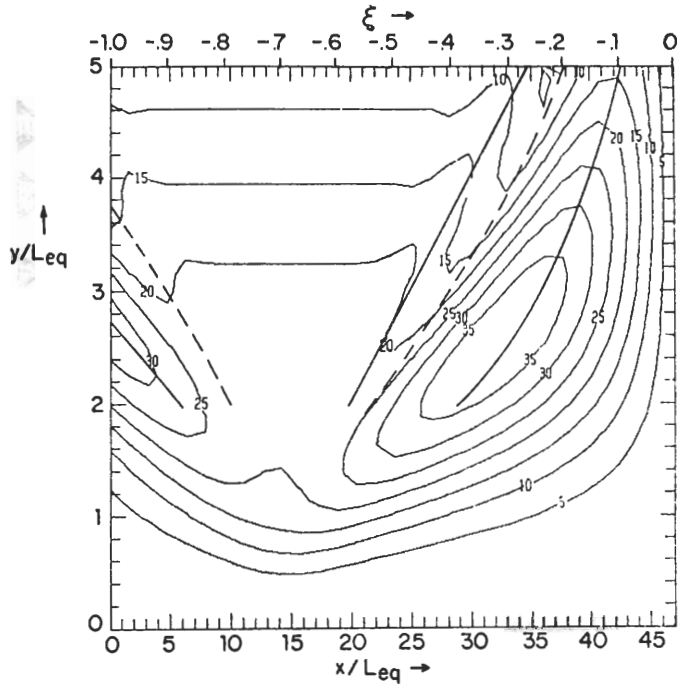

Figure 10. The Pacific Annual ($\phi = 1.13$) Anti-Symmetric Forcing Case for $\mu = .2$.
a) Amplitude of h/X_E. Contour interval is .05. Solid lines indicate maxima and dashed lines minima according to (44).

It is especially illuminating to compare the symmetric and anti-symmetric cases; examination of the general solution (19) shows that the major difference between the two cases resides in a term which consists of the Kelvin mode plus its eastern boundary Rossby reflections (Cane and Moore, 1981). In the low frequency limit ($\phi << 1$) both the symmetric and anti-symmetric cases had the height field *tilt* in phase with the forcing everywhere across the basin. For the anti-symmetric case, this was sufficient to insure that the height field itself was in phase with the forcing everywhere across the basin and thus be in equilibrium with the forcing. For the symmetric case, however, the presence of the aforementioned Kelvin wave term induces a phase variation of the height field with respect to the forcing so that the height field could no longer be said to be in equilibrium with the forcing. Only in the special case of forcings of large meridional scale (large values of the parameter $p = 2\phi\mu^{-1}$) was the height field itself in equilibrium with the forcing. Consequently, observations of the variations of dynamic topography *per se* are a more stringent test of theory than are observations of gradients.

This Kelvin wave term also makes itself felt in comparing the symmetric and anti-symmetric cases when ϕ is of order unity. The anti-symmetric case for $\phi > \pi/4$

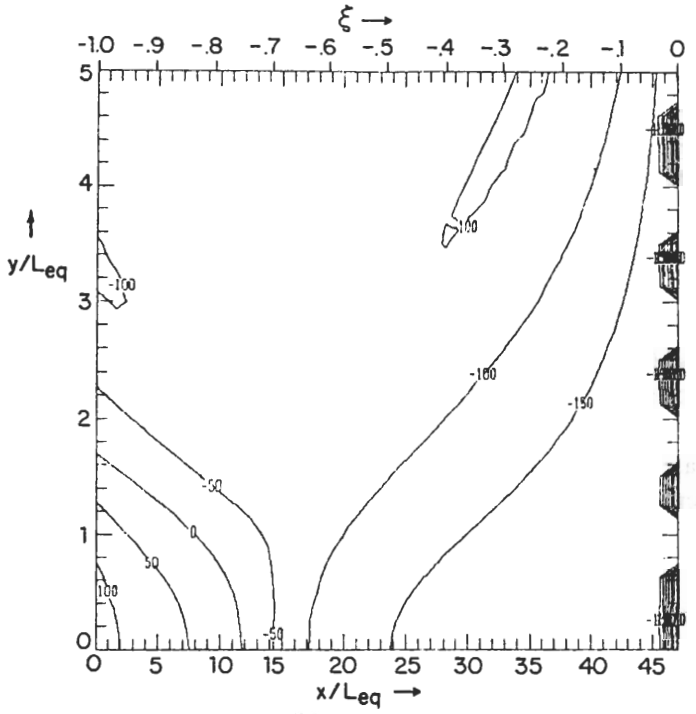

b) Phase of h with respect to the forcing (negative phases lead). Contour interval 50°. Hash on eastern boundary has no significance.

shows the characteristic focus-caustic-shadow zone structure predicted by Schopf *et al.* (1981) in their analysis of dispersion of Rossby waves. But a comparison of the symmetric *vs.* anti-symmetric case (e.g., Figs. 6a and 6b with Figs. 10a and 10b) shows considerably more structure in the symmetric case, with multiple maxima bounding the shadow zone and rapid phase variation within the shadow zone. Again, these additional complications can be traced to the term involving the Kelvin wave plus the boundary reflections, the first term in Eq. (35), which has the form of the third term but with $\mu = 0$. As Cane and Moore (1981) have shown, Rayleigh friction in this Kelvin term has the same effect as an x-dependent μ so that as friction is added, we may expect some of the additional structure due to the Kelvin term to be smoothed away.

The final consequence of the Kelvin term on the distinction between the symmetric and anti-symmetric cases is the effect on the phase. In all of the anti-symmetric cases, the phase variation was in such a direction as to indicate westward zonal phase velocities. In the symmetric cases where the Kelvin term was present, there were eastward phase velocities present somewhere. It is to be emphasized that the term involving the Kelvin wave plus its reflection is not confined to the vicinity

of the equator where the Kelvin mode has amplitude, but rather extends meridionally throughout the basin since the Kelvin mode excites all Rossby modes at the eastern boundary. Previous analyses of periodic response (e.g., White, 1977; Meyers, 1979; Schopf *et al.*, 1981) have treated the response solely in terms of Rossby waves without including the Kelvin wave and its Rossby reflections and thus cannot be valid for forcings with symmetric components. (An exception is Kindle, 1979.) In general, the periodic response is a complex superposition of Rossby waves, Kelvin waves and the eastern boundary reflections of the Kelvin waves. The phase of this response varies with both latitude and longitude even when the forcing has no spatial structure; it cannot be analyzed solely in terms of "annual Rossby waves" (a result that is supported by the aforementioned data studies).

In principle, a sum of Rossby modes, each term of which propagates westward, could involve eastward phase propagation. But in our forced symmetric problem, eastward phase propagation can be traced to the term involving the Kelvin mode plus its reflections, i.e. the term multiplying ρ in eq. (26). Therefore, in this forced problem, eastward phase propagation is not possible without the Kelvin mode. As noted in Section 4, for a symmetric annual forcing in the Atlantic, the response in thermocline depth variations showed a mean eastward phase speed of about 30 cm sec^{-1}, in agreement with Merle's (1980) analysis of equatorial Atlantic data. Our solution shows that almost all of the phase variation occurs in a region occupying about one third of the zonal extent of the basin centered at the "pivot point" one third of the way from the western side (Fig. 5b). This feature also agrees with Merle's data (see his Fig. 6 and note the actual positions of the heat content minima). Further, the pivot point in our solutions resembles the data in not being at the central longitude of the basin and in moving somewhat in time (cf. our Fig. 5a and Merle's Fig. 6b). The former characteristic has the consequence that the heat content of an equatorial band varies seasonally; not all heat is simply moved east-west; some is exchanged with higher latitudes.

In both the symmetric and anti-symmetric cases we considered the effects of the meridional scale of the forcing, especially near the equator. Since there is no equatorial response in the anti-symmetric case, most of the near-equatorial sensitivity to meridional scale exists in the symmetric case and we found, essentially by trial and error, that the amplitude response becomes independent of scale for meridional scales greater than ten degrees of latitude but that some phase variation persists for all meridional scales. A number of simulations of seasonal response have used realistic winds within a few degrees of the equator and then simply extended them uniformly in the meridional direction, a procedure that may give unrealistic results. (This may be the reason that Busalacchi and O'Brien (1980) obtain different results using a realistic wind field than when they duplicate Kindle's (1979) study.) This procedure has been justified by reference to McCreary's (1976)

El Niño study. In that work experiments with various wind forcings showed that only the symmetric component of the winds within three degrees of the equator affected the eastern boundary response. This result is correct for the *initial value* problem McCreary studied and is easily understood on theoretical grounds. For short times, only the initial wind-forced Kelvin wave reaches the eastern boundary. The amplitude of this wave is given by projecting the zonal wind forcing onto the Kelvin mode, a gaussian centered at the equator with a half width of about three degrees (for the first baroclinic mode). The seasonal response is a long time *equilibrium* response (the case studied in this paper). It allows time for Rossby waves at all latitudes to reach the western boundary and generate additional Kelvin waves which then propagate to the eastern boundary. Most studies of seasonal response have focused on eastern boundary effects (upwelling in the Gulf of Guinea, eastern Pacific thermocline displacement), precisely the region we have found to be most sensitive to the meridional scale of the winds.

Figure 1a shows that resonances exist for values of ϕ that are multiples of $\pi/2$ and that the amplitude of the response is enhanced in the neighborhood of these values. Taken at face value the data of Katz *et al.* (1977) suggest such an enhanced response: the amplitude of the annual component of the zonal wind is about half the mean while the variation of the zonal pressure gradient in the ocean is comparable to the mean. However, the values of ϕ appropriate to annual forcing in the Atlantic (.54 and .96 for the first and second baroclinic modes) are *not* near resonance. We believe that the available oceanographic data is not representative of the climatic mean because the only observations in the spring were from the Equalant expedition in 1963. That year was one of the most anomolous ever in the Atlantic (e.g., Katz *et al.*, 1977, Table 4) and the total absence of a zonal pressure gradient in that spring may be attributable to unusually weak zonal winds.

Throughout the analyses in this paper we have been struck by the fact that such simple forcings at a single frequency give such complicated and varied patterns of response. While there is some doubt about how much of this type of single layer, linear, inviscid, theory will survive the real world complications of inhomogeneous stratification, nonlinearities, realistic basic geometry, friction, and mean currents, it is worth pointing out the enhancements of periodic response ("foci") and diminutions of periodic response ("shadow zones") are present in linear theory and should be looked for in more realistic cases.

The complexity of our results has some disturbing implications for our prospects of understanding the low frequency deep jets observed in the equatorial oceans. The linear inviscid assumptions of our theory should hold for the deep ocean so that its low frequency response may be described by a linear superposition of vertical modes. Our results suggest that even if the low frequency forcing has a simple structure one would expect considerable spatial inhomogeneity in the deep ocean

response. In reality the deep ocean is forced by a combination of direct wind forcing, pumping from the nonlinear upper ocean and boundary effects. The structure of this forcing is neither simple nor well known.

On the basis of this linear inviscid theory we can draw some conclusions about the causes of the differences between equatorial thermocline response in the Atlantic and Pacific mentioned in the Introduction. The Pacific exhibits little annual variation of the thermocline relative to the mean, with the only marked changes occurring at the eastern end while the Atlantic shows substantial variations at all longitudes. Comparison of the equatorial response to symmetric winds for the Atlantic annual (Fig. 5c) and Pacific annual (Fig. 6c) cases indicates that the annual equatorial thermocline response should be *greater* in the Pacific and roughly of similar form. Since we therefore cannot attribute the difference to the basin size, our conclusion, based on linear, inviscid theory, must be that the difference in annual response in the two basins is attributable to the wind forcing. It is in fact the case that the zonal winds in the Atlantic have a stronger annual signal than the Pacific winds, especially in the near equatorial symmetric component. In contrast, the interannual variations of the winds are larger in the Pacific. Both factors make the Atlantic a better laboratory for studying the seasonal response and the Pacific a better laboratory for studying the interannual response of equatorial oceans.

Acknowledgments. We would like to thank our colleagues on the SEQUAL scientific panel for valuable discussions concerning the observational and theoretical aspects of equatorial periodic response. This work was supported by NASA Grant NGR 22-009-727 and NSF Grant OCE-7922046 at MIT and NASA Grant NGL 22-007-228 at Harvard.

APPENDIX 1: REVIEW AND NOTATION

The normalized scalar eigenfunctions on a meridionally unbounded equatorial β-plane are

$$\psi_n(y) = [\pi^{1/2}\, 2^n\, n!]^{-1/2}\, H_n(y) \exp[-y^2/2] \tag{A.1}$$

and satisfy the orthonormality condition

$$(\psi_n)_m = (\psi_m)_n = \delta_{nm} \tag{A.2}$$

where scalar projections are defined by

$$(\ \ )_n = \int_{-\infty}^{\infty} (\ \ )\psi_n(y)\, dy\,. \tag{A.3}$$

A projection that repeatedly occurs is that of y:

$$(y)_{2n+1} \equiv 2\pi^{1/4}\, \alpha_{2n+1} = 2\pi^{1/4}\, [2^n n!]^{-1}\, [(2n+1)!]^{1/2}\,, \tag{A.4}$$

where only odd projections exist by the symmetry properties of the eigenfunctions. Using Stirling's formula in (A.4), the α_{2n+1}'s are easily seen to go as $n^{1/4}$ for large n.

Along the equator $y = 0$, only symmetric functions have non-zero values and these are related to the α's by

$$\psi_{2n}(0) = (-1)^n\, [\pi^{1/2}\, (2n+1)]^{-1/2}\, \alpha_{2n+1}\,. \tag{A.5}$$

Normalized Kelvin and Rossby vector functions are defined by (the upper component refers to u, lower to h and super T means transpose)

$$\mathbf{M}_K = 2^{-1/2}\,[\psi_0, \psi_0]^T \tag{A.6a}$$

and

$$\mathbf{R}_n = [4n(n+1)]^{-1}\,[-(2n+1)\psi'_n - y\psi_n,\ (2n+1)y\psi_n + \psi'_n]^T \tag{A.6b}$$

$$= \frac{1}{2\sqrt{2}} \begin{bmatrix} (n+1)^{-1/2}\psi_{n+1} - n^{-1/2}\psi_{n-1} \\ (n+1)^{-1/2}\psi_{n+1} + n^{-1/2}\psi_{n-1} \end{bmatrix} . \tag{A.6c}$$

Both the Kelvin and Rossby functions (A.6a) and (A.6b) have their u velocities in geostrophic balance with their height fields, i.e., $yu + h_y = 0$. They are, in addition, mutually orthogonal,

$$[\mathbf{R}_n, \mathbf{M}_K] = [\mathbf{M}_K, \mathbf{R}_n] = 0 \tag{A.7a}$$

and satisfy the normalization conditions

$$[\mathbf{M}_K, \mathbf{M}_K] = 1 \text{ and } [\mathbf{R}_n, \mathbf{R}_m] = (2n+1)\,(4n\,(n+1))^{-1}\delta_{nm} \tag{A.7b}$$

where

$$[\mathbf{A}, \mathbf{B}] \equiv \int_{-\infty}^{\infty} [A_u B_u + A_h B_h]\, dy\ .$$

APPENDIX 2: SOME EXACT SUMS

Consider the vector sum

$$\mathbf{L}\,(y,c) = c^{-1}\mathbf{M}_K + 2 \sum_{n=0}^{\infty} \alpha_{2n+1}\mathbf{R}_{2n+1}c^{2n+1}\ . \tag{A.8}$$

By using the explicit forms of $\mathbf{M}_K$ and $\mathbf{R}_{2n+1}$ in (A.6) as in Cane and Moore (1981), the definition of α_{2n+1} in (A.4), and by rearranging the sum, (A.8) can be rewritten

$$\mathbf{L}\,(y,c) = R\,(y,c)\,[1 - c^2,\ 1 + c^2]^T \tag{A.9}$$

where

$$R\,(y,c) = 2^{-1/2}c^{-1} \sum_{n=0}^{\infty} (2n+1)^{-1/2}\alpha_{2n+1}\psi_{2n}\,(y)c^{2n}\ . \tag{A.10}$$

The integral representation for the Hermite function

$$H_{2n}\,(y) = \pi^{-1/2}2^{2n+1} \exp\,[y^2] \int_0^{\infty} (-1)^n t^{2n} \exp\,[-t^2] \cos 2yt\, dt \tag{A.11}$$

can now be used in (A.10) and interchanging the integral and the sum yields

$$R\,(y,c) = 2\pi^{-3/4} \exp\,[y^2/2] \int_0^{\infty} \exp\,[-t^2] \cos 2yt \sum_{n=0}^{\infty} [n!]^{-1}\,(-1)^n t^{2n} c^{2n}\, dt\ .$$

The sum is simply $\exp\,[-c^2t^2]$ and the integral can be performed using

$$\int_0^{\infty} \exp\,[-\beta t^2] \cos bt\, dt = (\pi/4\beta)^{1/2} \exp\,[-b^2/4\beta]$$

(Gradshteyn and Rhyzhik, 1965; Eq. 3.896,4) to yield, finally,

$$R\,(y,c) = c^{-1}\,(2\pi^{1/2})^{-1/2}\,(1+c)^{-1/2}\exp\,[y^2\,(c^2-1)/2\,(c^2+1)]\ . \tag{A.12}$$

As a special case, $c = 1$ reduces to a sum used extensively in Cane and Sarachik (1977)

$$\mathbf{L}\,(y,1) = \mathbf{M}_K + 2\sum_{n=0}^{\infty}\alpha_{2n+1}\mathbf{R}_{2n+1} = \pi^{-1/4}\,[0,1]^T\ . \tag{A.13}$$

Putting $c = \exp\,[2i\phi\xi]$ produces the form used in the body of the text (e.g, Eq. (21)).

An important scalar sum is derived by considering the h component of $\mathbf{L}\,(y,c)$ at $y = 0$. Using the explicit expression for $\mathbf{R}_{2n+1}\,(y)$ in (A.6c) and evaluating it on the equator using (A.5) yields

$$c^{-1} + \sum_{n=0}^{\infty}(-1)^n\,[\alpha_{2n+1}]^2\,(2n+1)^{-1}\,(2n+2)^{-1}c^{2n+1} = (1+c^2)^{1/2}c^{-1} \tag{A.14}$$

where the sum $R\,(0,c)$ has been used for the right-hand side of (A.13). Finally, noting that $(-1)^n = -i\,(i)^{2n+1}$, defining $\gamma_n = [\alpha_n]^2 n^{-1}\,(n+1)^{-1}$, and redefining $c \to ic$ yields the scalar sum

$$S\,(c) = \sum_{n=0}^{\infty}\gamma_{2n+1}c^{2n+1} = c^{-1}\,[1-(1-c^2)^{1/2}]\ . \tag{A.15}$$

The special case $S\,(1) = 1$ was already noted in the Appendix to Cane and Sarachik (1977).

An anti-symmetric scalar sum

$$Q\,(y,c) = 2\pi^{1/4}\sum_{n=0}^{\infty}\alpha_{2n+1}\psi_{2n+1}c^{2n} \tag{A.16}$$

can be summed by methods almost identical to those leading to the sum for $R\,(y,c)$ with the result

$$Q\,(y,c) = y\left(\frac{2}{1+c^2}\right)^{3/2}\exp\left[\frac{y^2}{2}\left(\frac{c^2-1}{c^2+1}\right)\right]\ . \tag{A.17}$$

When $c = 1$, (A.16) and (A.17) are just the expansion for y.

APPENDIX 3: MATHEMATICAL MANIPULATIONS

For the symmetric forcing case, $F = \exp\,[-1/2\mu y^2]$, discussed in Sec. 4 of the text, the necessary projections of the forcing may be taken analytically. Since the forcing is symmetric with respect to the equator, only odd values of n need be considered in the Rossby projection r_n so that

$$r_{2n+1} = -\frac{2\pi^{1/4}\,\alpha_{2n+1}}{(1+\mu)^{3/2}}\left[\frac{1-\mu}{1+\mu}\right]^n\left[\mu+\frac{1}{4n+3}\right] \tag{A.18a}$$

and the Kelvin projection is

$$d_K = \pi^{1/4}\,(1+\mu)^{-1/2}\ . \tag{A.18b}$$

Then, the functions needed in the general solution (19) and (20) become

$$B_N(i\phi) = \frac{-\pi^{1/4}}{(1+\mu)^{3/2}} \sum_{n=0}^{N} \gamma_{2n+1} \left[\frac{1-\mu}{1+\mu}\right]^n \left[\mu + \frac{1}{4n+3}\right] [1-\exp[-i\phi(4n+3)]] \tag{A.19a}$$

and

$$S_N(\exp[-2i\phi]) = \sum_{n=0}^{N} \gamma_{2n+1} \exp[-(2n+1)2i\phi] \tag{A.19b}$$

where

$$\gamma_n = (\alpha_n)^2 [n(n+1)]^{-1} .$$

We wish to show now that it is a good approximation in (A.19a) and (A.19b) to take $N \to \infty$. From the explicit expression for α_n in (A.4) it is seen that $\alpha_n \to n^{1/4}$ for large n so that $\gamma_n \to n^{-3/2}$ for large n. Thus in the expression for $S_N(\exp[-2i\phi])$, for example, as long as 2ϕ is not near 0 or a multiple of π, the series for both the real and imaginary part will have converged well below N and little error is made by continuing to sum to infinity. When ϕ is near zero, the terms in the imaginary part of S_N are $\gamma_{2n+1} \sin(2n+1)\phi$ and will go as $n^{-1/2}$ for $(2n+1) \ll \phi^{-1}$ and $n^{-3/2}$ for $(2n+1) \gtrsim \phi^{-1}$. The condition that $S_N \to \infty$ be a good approximation to S_N is that the terms of the series be in the $n^{-3/2}$ region for $n \leqslant N$. Since $2N+1 \sim \phi^{-2}$, this condition is simply that $1 < \phi^{-1}$ so that for low frequencies $\mathrm{Lim}_{N\to\infty} S_N$ is always a good approximation to S_N. Another way of saying this is that as the frequency gets small, the number of terms needed for convergence increases as ϕ^{-1}, while the number of terms of the series (N) increases as ϕ^{-2} so that for small enough ω (or ϕ) the sum of N terms will always include the convergent region and the sum can then safely be extended to infinity. The limit of $S_N(\exp[-2i\phi])$ can be summed using the sum (A.15) in the Appendix and is simply

$$\begin{aligned} \lim_{N\to\infty} S_N(\exp[-2i\phi]) &= S(\exp[-2i\phi]) \\ &= \exp[2i\phi] - (2i\sin 2\phi)^{1/2} \exp[i\phi] . \end{aligned} \tag{A.20}$$

The expression for $B_N(i\phi)$ can similarly be extended to $N \to \infty$ using arguments similar to those for S_N. Again the scalar sum in (A.15) of Appendix 2 can be used to explicitly evaluate these infinite sums. Thus in $B(i\phi) = \mathrm{Lim}_{N\to\infty} B_N(i\phi)$ the sum

$$\sum_{n=0}^{N} \gamma_{2n+1} \left[\frac{1-\mu}{1+\mu}\right]^n [1-\exp[-i\phi(4n+3)]] \tag{A.21}$$

is evaluated in terms of the S function of Appendix 2 to be

$$\begin{aligned} &\left(\frac{1+\mu}{1-\mu}\right)^{1/2} \left\{ S\left[\left(\frac{1-\mu}{1+\mu}\right)^{1/2}\right] - \exp[i\phi]\, S\left[\left(\frac{1-\mu}{1+\mu}\right)^{1/2} \exp[-2i\phi]\right] \right\} \\ &\quad = \left(\frac{1+\mu}{1-\mu}\right) \left[1 - \left(\frac{2\mu}{1+\mu}\right)^{1/2} - \exp[i\phi] + \left(\frac{2}{1+\mu}\right)^{1/2} q(\mu, -\phi)\right] \end{aligned} \tag{A.22}$$

where

$$q(\mu,\phi) = [\mu\cos 2\phi - i\sin 2\phi]^{1/2} . \tag{A.23}$$

Similarly, the sum

$$\sum_{n=0}^{\infty} \frac{\gamma_{2n+1}}{4n+3} \left[1 - \exp\left[-i\phi\,(4n+3)\right]\right] \left(\frac{1-\mu}{1+\mu}\right)^n$$

$$= i \int_0^{\phi} \sum_{n=0}^{\infty} \gamma_{2n+1} \left(\frac{1-\mu}{1+\mu}\right)^n \exp\left[-i\phi'\,(4n+3)\right] d\phi'$$

$$= i \int_0^{\phi} \exp\left[-i\phi'\right] \left(\frac{1+\mu}{1-\mu}\right)^{1/2} S\left[\left(\frac{1-\mu}{1+\mu}\right)^{1/2} \exp\left[-2i\phi'\right]\right] d\phi'$$

$$= i \left(\frac{1+\mu}{1-\mu}\right)^{1/2} \int_0^{\phi} \left[\exp\left[i\phi'\right] - 2^{1/2}\,(1+\mu)^{-1/2}\, q\,(\mu, -\phi')\right] d\phi' \,. \tag{A.24}$$

Combining (A.20), (A.22), and (A.24) in the expression (A.19a) for B yields the explicit expression

$$B\,(i\phi) = \pi^{1/4}\,(1+\mu)^{-1/2}\,(1 - \exp\left[i\phi\right])$$

$$+ \pi^{1/4}\, 2^{1/2}\,(1-\mu^2)^{-1} \left[\mu^{3/2} - \mu q\,(\mu, -\phi) + i \int_0^{\phi} q\,(\mu, -\phi')\, d\phi'\right] . \tag{A.25}$$

Combining (A.21) with (A.20) in the definition (20) for ρ finally yields

$$d_K \rho\,(i\phi) \equiv \operatorname*{Lim}_{N\to\infty} \pi^{1/4}\,(1+\mu)^{-1/2}\,\rho_N\,(i\phi)$$

$$= \pi^{1/4}\,(1-\mu^2)^{-1}\,[i \sin\, 2\phi]^{-1/2} \left[\mu^{3/2} - \mu q\,(\mu, -\phi) + i \int_0^{\phi} q\,(\mu, -\phi')\, d\phi'\right] . \tag{A.26}$$

Now, having obtained the scalar function ρ and having already summed (in Eq. (21)) the vector terms multiplying ρ in Eq. (19), we proceed to sum the Rossby terms in (19) in the limit that $N \to \infty$. To do this we need the sum

$$\sum_{n=0}^{\infty} \alpha_{2n+1} \left(\frac{1-\mu}{1+\mu}\right)^n \left[1 - \exp\left[i\phi\xi\,(4n+3)\right]\right] \mathbf{R}_{2n+1} \,.$$

This can be written in terms of the vector sum $\mathbf{L}\,(y,c)$ defined in (A.8) of Appendix 2 as

$$\frac{1}{2} \left(\frac{1+\mu}{1-\mu}\right)^{1/2} \left\{ - \left(\frac{1+\mu}{1-\mu}\right)^{1/2} \mathbf{M}_K + \mathbf{L}\left(y, \left(\frac{1-\mu}{1+\mu}\right)^{1/2}\right)\right.$$

$$\left. - \left(\frac{1+\mu}{1-\mu}\right)^{1/2} \exp\left[-i\phi\xi\right] \mathbf{M}_K + \exp\left[i\phi\xi\right] \mathbf{L}\left(y, \left(\frac{1-\mu}{1+\mu}\right)^{1/2} \exp\left[2i\phi\xi\right]\right)\right\} . \tag{A.27}$$

Similarly,

$$\sum_{n=0}^{\infty} \alpha_{2n+1} \left(\frac{1-\mu}{1+\mu}\right)^n \frac{1}{4n+3} \left[1 - \exp\left[i\phi\xi\,(4n+3)\right]\right] \mathbf{R}_{2n+1}$$

$$= -i \int_0^{\phi\xi} \sum_{n=0}^{\infty} \alpha_{2n+1} \left(\frac{1-\mu}{1+\mu}\right)^n \exp[i\zeta(4n+3)]\, \mathbf{R}_{2n+1}\, d\zeta$$

$$= -\frac{i}{2}\left(\frac{1+\mu}{1-\mu}\right)^{1/2} \int_0^{\phi\xi} \left\{ -\left(\frac{1+\mu}{1-\mu}\right)^{1/2} \exp[-i\zeta]\, \mathbf{M}_K \right.$$

$$\left. + \exp[i\zeta]\, \mathbf{L}\left(y, \left(\frac{1-\mu}{1+\mu}\right)^{1/2} \exp[2i\zeta]\right)\right\} d\zeta \,. \qquad \text{(A.28)}$$

Finally, collecting all the terms in (19) together and using the form of $\mathbf{L}(y,c)$ given in (A.9) and (A.12) gives the explicit form for the response to the forcing $\exp[-1/2\ \mu y^2 + i\omega t]$. This is given in eq. (26) of the main body of the text.

For the anti-symmetric forcing $y \exp[-1/2\ \mu y^2 + i\omega t]$ discussed in Sec. 5 of the text, the projections of this forcing may be taken explicitly as:

$$r_{2n} = -2^{1/2}\pi^{1/4} \frac{8\mu}{1-\mu^2}\left(\frac{1-\mu}{1+\mu}\right)^n \qquad \alpha_{2n+1} \frac{n(2n+1)^{1/2}}{4n+1} \,. \qquad \text{(A.29)}$$

If we extend the sum N to infinity in (41) using the same approximation as before, and use the explicit form for the Rossby mode given in (A.6b) then the solution can be written in terms of two infinite series:

$$\mathbf{u} = -\frac{\exp[i\omega t]}{i\omega} \frac{2\mu}{1-\mu^2} (1+\mu)^{1/2} \left\{ I_1 \begin{bmatrix} 1 \\ 1 \end{bmatrix} + \frac{1}{2}\frac{(1-\mu)}{(1+\mu)} I_2 \begin{bmatrix} -1 \\ 1 \end{bmatrix}\right\} \qquad \text{(A.30)}$$

where

$$I_1 = 2\pi^{1/4} \sum_{n=0}^{\infty} \alpha_{2n+1} \frac{n}{4n+1}\left(\frac{1-\mu}{1+\mu}\right)^n \psi_{2n+1}[1 - \exp[i\phi\xi(4n+1)]] \qquad \text{(A.31a)}$$

and

$$I_2 = 2\pi^{1/4} \sum_{n=0}^{\infty} \alpha_{2n+1} \frac{2n+3}{4n+5}\left(\frac{1-\mu}{1+\mu}\right)^n \psi_{2n+1}[1 - \exp[i\phi\xi(4n+5)]] \,. \qquad \text{(A.31b)}$$

Using the identities

$$\frac{n}{4n+1} = \frac{1}{4}\left[1 - \frac{1}{4n+1}\right]$$

and

$$\frac{2n+3}{4n+5} = \frac{1}{2}\left[1 + \frac{1}{4n+5}\right]$$

both series can be written in terms of the single series

$$P(\mu,\phi) = 2\pi^{1/4} \sum_{n=0}^{\infty} \alpha_{2n+1} \left(\frac{1-\mu}{1+\mu}\right)^n \psi_{2n+1} \exp[i\phi\xi(4n+3)] \qquad \text{(A.32)}$$

as

$$I_1 = 4^{-1} \left\{ P(\mu,0) - P(\mu,\phi\xi)\exp[-2i\phi\xi] + i\int_0^{\phi\xi} P(\mu,\zeta)\exp[-2i\zeta]\, d\zeta \right\} \qquad \text{(A.33a)}$$

and

$$I_2 = 2^{-1} \left\{ P(\mu,0) - P(\mu,\phi\xi)\exp[2i\phi\xi] - i\int_0^{\phi\xi} P(\mu,\zeta)\exp[2i\zeta]\, d\zeta \right\} . \qquad \text{(A.33b)}$$

The series $P(\mu,\phi)$ can be summed explicitly in terms of the anti-symmetric scalar sum Q given in (A.17):

$$P(\mu,\phi) = \exp[3i\phi]Q\left(y, \left(\frac{1-\mu}{1+\mu}\right)^{1/2} \exp[2i\phi]\right)$$

$$= y(1+\mu)^{3/2} r^{-3}(\mu,\phi) \exp\left[\frac{1}{2} y^2 \eta(\mu,\phi)\right]. \qquad \text{(A.34)}$$

Finally, combining (A.30), (A.33), and (A.34) yields the final result given in Eq. (42) in the main body of the text.

REFERENCES

Bender, C. M. and S. A. Orszag. 1978. Advanced Mathematical Methods for Scientists and Engineers. McGraw Hill, 593 pp.

Busalacchi, A. J. and J. J. O'Brien. 1980. The seasonal variability in a model of the tropical Pacific. J. Phys. Ocean., *10*, 1929–1951.

Cane, M. A. and D. W. Moore. 1981. A note on low frequency equatorial basin modes. J. Phys. Oceanogr., in press.

Cane, M. A. and E. S. Sarachik. 1976. Forced baroclinic ocean motions. I. The linear equatorial unbounded case. J. Mar. Res., *34*, 629–665.

—— 1977. Forced baroclinic ocean motions. II. The linear equatorial bounded case. J. Mar. Res., *35*, 395–432.

—— 1979. Forced baroclinic ocean motions. III. The linear equatorial basin case. J. Mar. Res., *37*, 355–398.

Gradshteyn, I. S. and I. M. Ryzhik. 1965. Tables of Integrals, Series, and Products, Academic Press, 1086 pp.

Katz, E. J. and Collaborators. 1977. Zonal pressure gradient along the equatorial Atlantic. J. Mar. Res., *35*, 293–307.

Kindle, J. C. 1979. Equatorial Pacific Ocean variability—seasonal and El Niño time scales. Florida State University Doctoral Dissertation.

McCreary, J. 1976. Eastern tropical ocean response to changing wind systems with application to El Niño. J. Phys. Ocean., *6*, 632–645.

Merle, J. 1980. Seasonal heat budget in the equatorial Atlantic Ocean. J. Phys. Ocean., *10*, 464–469.

Meyers, G. 1979a. Annual variation in the slope of the 14°C isotherm along the equator in the Pacific Ocean. J. Phys. Ocean., *9*, 885–891.

—— 1979b. On the annual Rossby wave in the tropical North Pacific Ocean. J. Phys. Ocean., *9*, 663–674.

Moore, D. W. 1968. Planetary-gravity waves in an equatorial ocean. Harvard University Doctoral Dissertation.

Pedlosky, J. 1965. A note on the western intensification of the oceanic circulation. J. Mar. Res., *23*, 207–210.

Philander, S. G. H. 1979. Variability of the tropical oceans. Dyn. Atmos. and Oceans, *3*, 191–208.

Philander, S. G. H. and R. R. Pacanowski. 1981. The response of equatorial oceans to periodic forcing. J. Geophys. Res., *86*, 1903–1916.

Schopf, P., D. L. T. Anderson and R. Smith. 1981. Beta-dispersion of low frequency Rossby waves. Dyn. Atmos. and Oceans, *5*, 187–214.

Tsuchiya, M. 1979. Seasonal variation of the equatorial zonal geopotential gradient in the eastern Pacific Ocean. J. Mar. Res., *37*, 399–407.

White, W. B. 1977. Annual forcing of baroclinic long waves in the tropical North Pacific Ocean. J. Phys. Ocean., *7*, 50–61.

Received: *9 October, 1980*; revised: *20 July, 1981.*